STACKING SEQUENCES OPTIMIZATION OF LAMINATED COMPOSITES FOR MAXIMUM BUCKLING STRENGTH BY STOCHASTIC SEARCH METHODS

A Thesis Submitted to
the Graduate School of
İzmir Institute of Technology
in Partial Fulfillment of the Requirements for the Degree of

MASTER OF SCIENCE

in Mechanical Engineering

by
Gökay ADABAŞI

December 2020
İZMİR

ACKNOWLEDGEMENTS

First and foremost, I would like to express my endless thanks to my academic advisor Assoc. Prof. Dr. H. Seçil Artem, who has always supported me, who has been working hard on me for about 7 years. She never withheld her knowledge from me, rather she worked patiently to teach something more. I will always be proud to work with her and to be her student.

I would like to thank Assoc. Prof. Dr. Levent Aydın, Asst. Prof. Dr. Arda Deveci, Ozan Ayakdaş, M.Sc., and Alihan İmamoğlu, who are members of the Optimization Modeling and Applied Math Research Group (OMA-RG). I special thanks to my close friend from the ARTEM research group, A. Harun Sayı, M.Sc., who always helped to share his knowledge with me. At the same time, I would like to express my gratitude to my dear colleagues Baran Gülbaş, Alican Arslan, and Ceren Karadoğan who have always supported me.

I should state that I am grateful to my mother, my father, and grandparents, Dilek Adabaşı, Ercan Adabaşı, Kadriye Adabaşı, and Hüseyin Adabaşı, who supported me in my nearly 21 years of education under all circumstances, who always stood behind me and who did not spare their financial and moral support.

I would like to convey another thanks to the valuable professors of Izmir Institute of Technology. I am grateful to the worthy professors of the Department of Mechanical Engineering, who always supported me. By studying IZTECH, I improved myself both personally and academically. I am very lucky to be a part of this special community.

I would like to express my last thanks to volleyball, which has been in my life for nearly 17 years and will always continue as my greatest passion and greatest pleasure.

ABSTRACT

STACKING SEQUENCES OPTIMIZATION OF LAMINATED COMPOSITES FOR MAXIMUM BUCKLING STRENGTH BY STOCHASTIC SEARCH METHODS

Based on materials developed and made available by humans, there are materials that will serve their purpose. Using lighter materials, especially in the field of aviation and space, significantly reduces the costs. However, lightness is not the only feature required in materials. In addition, the physical and mechanical properties of the materials must be at the desired level. Knowing the buckling load capacity of composite materials, which are widely used, is also very important in determining the material properties. Accordingly, an important focus of this thesis is to examine the behavior of different materials against the same loading; the other is to examine the increase in the critical buckling load factor although they have the same geometric structure. Critical buckling load factor is considered when performing the buckling analysis. The mechanical behavior of composite materials used by considering the factors of critical buckling load factor has been investigated and discussed. Different optimization methods have been used while making the optimum design of different composite materials with 48 and 64 layers in total. The verification of mechanical properties of materials was made with the help of coding. Subsequently, the referenced articles were verified to prove the accuracy of this code. Optimization was carried out by using material properties information from reference articles and verifying the code. As a result, considering the buckling strength of different layered composite materials, it has been found that the optimum designs depend on the load, load ratio, and plate aspect ratio.

ÖZET

MAKSIMUM BURKULMA DAYANIMI İÇİN TABAKALI KOMPOZİTLERİN STOKASTİK YÖNTEMLERLE TABAKA DİZİMLERİNİN OPTİMİZASYONU

İnsanlar tarafından geliştirilip kullanıma sunulan materyallerin temelinde amacına uygun olarak hizmet edecek malzemeler vardır. Özellikle havacılık ve uzay sektöründe daha hafif malzemelerin kullanılması maaliyetleri ciddi anlamda düşürmektedir. Fakat malzemelerde aranan tek özellik hafif olması değildir. Bunun yanında malzemelerin fiziksel ve mekanik özelliklerinde istenilen düzeyde olması gereklidir. Malzeme özelliklerinin belirlenmesinde ve özellikle kullanımı yaygınlaşan kompozit malzemelerin burkulma yükü kapasitesinin bilinmesi malzemelerin tasarımı için de çok önemlidir. Bu doğrultuda, bu tezin önemli odak noktalarından biri, farklı malzemelerin aynı yüklemeye karşı davranışını incelemektir; diğeri ise aynı geometrik yapıya sahip olmasına rağmen kritik burkulma yük faktöründeki artışı incelemektir. Burkulma analizi yapılırken, kritik burkulma yük faktörü dikkate alınmıştır. Kritik burkulma yük faktörünün etkenleri göz önüne alınarak kullanılan kompozit malzemelerin mekanik davranışlarının incelenmesi araştırılmış. Toplamda 48 ve 64 tabakalı olan farklı kompozit malzemelerin optimum tasarımı yapılırken farklı optimizasyon yöntemleri kullanılmıştır. Malzemelerin mekanik özelliklerinin doğrulaması kodlama yardımıyla yapılmıştır. Sonrasında bu kodun doğruluğu kanıtlamak için referans alınan makalelerin doğrulaması yapılmıştır. Referans makalelerden alınan malzeme bilgileri kullanılarak ve kodun doğrulaması sağlanarak optimizasyon gerçekleştirilmiştir. Sonuç olarak, tabakalandırılmış farklı kompozit malzemelerin burkulma dayanımı dikkate alınarak optimum tasarımlarının yük, yük oranı, plaka en-boy oranına bağlı olduğu bulunmuştur.

TABLE OF CONTENTS

LIST OF FIGURES

Figures **Page**

LIST OF TABLES

Tables **Page**

Tables **Page**

Tables **Page**

CHAPTER 1

INTRODUCTION

1.1. Literature Survey

Today, with the developing technology, in many areas such as the electrical and electronics industry, aviation industry, automotive industry, and construction sector, instead of traditional metals such as steel, composite materials with a high strength / weight ratio started to be used. The importance of composite materials has increased day by day, and accordingly, the work to produce and develop suitable composite that meets the need has gained speed. The variety of fibers used as reinforcement for composite materials; provides convenience in terms of meeting the properties such as high strength, high hardness, low density (lightness), and low cost required from composite materials. For this reason, different composites have been obtained by using different fibers together in order to meet the needs better. Composites are made from at least two different types of materials. Composites have a variety of uses, one of which is in hybrid composites. For example, the advantage of hybrid composites obtained by using graphite/epoxy and flax/epoxy together as reinforcing elements has been effective in the widespread use of hybrid composites consisting of graphite/epoxy and flax/epoxy. The widespread use of hybrid composites has made this issue more and more important every day. However, composite materials have started to be used instead of different materials. The main reason can be said because of weight reduction studies. For example, instead of steel and its derivatives, glass/epoxy or glass/polyester can be considered in accordance with their usage areas. Likewise, it is seen that the use of carbon/epoxy instead of aluminum has increased. However, one of the most important issues to be considered during these examinations is sprain. Some of these studies are as follows.

One of the first buckling studies is done on behalf of different types of composites by Duffy and Adali (1990). It is a successful work that has managed to be the reference of most studies. It presents the concept of hybrid symmetric laminated plates consisting of a high-stiffness surface and core layers of low-stiffness. The maximization of buckling load is done over a discrete set of ply angles in the first problem. In the second problem,

for a given buckling load to minimize the material expense, the minimum number of high-stiffness plies is calculated. To define the stacking sequence, Boolean variables are added. The solution to the problem of linear optimization yields an optimal stacking sequence. For different problem parameters, such as the aspect ratio of the laminate and the number of plies, the effects of hybridization are investigated. With upper bound constraints on the effect of bending- twisting coupling constraints, the optimum designs are obtained. Results for hybrid graphite/glass-epoxy are provided (Duffy and Adali 1990).

To optimize the stacking sequence of a composite laminate for buckling load maximization, the use of a genetic algorithm is being studied by Le Riche and Haftka (1993). Various genetic parameters are optimized by computational tests, including population size, mutation probability, and crossover probability. It is suggested that a new genetic operator, permutation, is efficient in reducing the cost of genetic search. Results for a graphite-epoxy plate are obtained, first when only the buckling load is taken into account, and then when restrictions on ply contiguity and strain failure are applied. The effect of the penalty parameter imposing the constraint of contiguity on the genetic search is studied (Le Riche and Haftka 1993).

Erdal and Sonmez (2005) proposes a method for identifying globally optimal designs for two-dimensional composite materials subject to static in-plane loads for which buckling is the critical failure mode. The goal is to optimize the potential of laminated composites for the buckling load. An optimized design of the simulated annealing algorithm, which is direct simulated annealing (DSA), has been used for this purpose. Fiber orientation was used as a design variable in each sheet. A computer code was created and the results over many load cases were gathered (Erdal and Sonmez 2005).

Onal (2006) research analyzes the buckling study of symmetric and antisymmetric cross-ply laminated hybrid composite plates with an inclined crack subjected to uniform compression. In the numerical solution, the first-order shear deformation principle in combination with the multi - objective energy approach is used. The impacts on the buckling loads are examined by crack scale, crack inclination angle, and lay-up sequences (Onal 2006).

The structural optimization of composite laminates is carried out using a genetic algorithm for optimum buckling load capacity by Soykasap and Karakaya (2007). The composite plate under consideration is a graphite/epoxy 64-ply laminate, which is simply supported on four sides and is subject to static compressive loads in the plane. Using 2-

ply stacks, the critical buckling loads are calculated for multiple load cases and various plate aspect ratios (Soykasap and Karakaya 2007).

For the optimal stacking sequence of a composite panel, which is supported on four sides and is subject to biaxial in-plane compressive loads, the genetic algorithm and generalized pattern search algorithm are used in Karakaya and Soykasap (2009). In the area of local optima, the problem has multiple global optimal configurations. The 64-ply laminate made from graphite/epoxy is the composite plate under consideration. The laminate, consisting of two laminate sequences, is known to be symmetrical and balanced. The critical buckling loads for many combinations of load case and plate aspect ratio are ply stacks with distinct fiber angles of 0_2, ± 45, and 90_2 maximized and are contrasted with published data. In terms of capability to define global optima, the performance of both algorithms is compared. Genetic algorithms have been shown to be useful for problems with global optima (Karakaya and Soykasap 2009).

Aymerich and Serra (2008) demonstrates the application of meta - heuristic ant colony optimization (ACO) to the lay-up design of laminated panels to optimize buckling load with strength restraints. In order to characterize the computational efficiency and the quality of results given by the developed ACO algorithm, a specific problem previously studied by various researchers using genetic algorithms (GA) and Tabu search (TS) was chosen as a test case (Aymerich and Serra 2008).

The goal of Yeter et al. (2014) is to determine the effect of hybridization on composite plates' buckling behavior consisting of symmetrical and unsymmetrical ply orientations, different cutout shapes, and combination of length/thickness. Carbon, S-glass, and Aramid fibers are used with epoxy resin as reinforcement. Experimental studies are conducted to see the impact on bucking loads with symmetrical and unsymmetrical ply orientations with different fiber combinations. Numerical studies are also conducted to see the impacts on the buckling loads of the length/thickness ratio and different cutout shapes. It is concluded that the buckling effects of the composite plates are influenced by stiffness and shear properties. The buckling strength is also improved by fibers with higher stiffness and higher shear properties in the upper layers (Yeter, Erkliğ, and Bulut 2014).

An optimization technique is suggested by Deveci et al. (2016) to find the optimal stacking sequence designs of laminated composite plates for optimum buckling resistance at different fiber angle areas. A hybrid algorithm that combines the genetic algorithm and the reflective trust zone algorithm is used in optimization to achieve higher performance

and increase the efficiency of solutions. As a novelty, as nonlinear function constraints that provide more reliable and workable outcomes, the Puck fiber and fiber-to-fiber error criteria are specifically applicable to optimization issues. By comparing the individual outputs of the genetic and confidence zone reflection algorithms with the test problems in the literature, the efficiency of the hybrid algorithm was demonstrated (Deveci, Aydin, and Seçil Artem 2016).

The buckling study of the inter-ply hybrid composite plate formed by the combination of one natural and two synthetic unidirectional fabrics and epoxy resin is mainly evaluated by Ahmad and Rajput (2020). The finite element approach is used to predict the buckling action of the symmetrical and un-symmetrical ply orientation composite plate and the ply orientations of FCA, FAC, CFA, CAF, AFC, and ACF (Ahmad and Rajput 2020).

The refined plate theory discusses this article, considering the simpler method of governing differential equations used to solve buckling analysis of laminated composite plates by Wankhade and Niyogi (2020). With recent developments in plastic science, these laminated composites are also used in structural applications. This led to the development of a modern composite to preserve compressive in-plane loading with improved properties. Laminated composites can be vulnerable to buckling under compressive loads and/or due to thin build-up. Therefore, the analysis of buckling characteristics of laminated composites is appealing and testing is now needed for days. Very few literatures with different boundary conditions on buckling characteristics of laminated composite plate are available. Therefore, with a cross-ply lamination system of plates with certain boundary conditions, this research explores buckling actions of laminated composite structures (Wankhade and Niyogi 2020).

Savran and Aydin (2018) is one of the main reference articles for this thesis study because of the material used. The current paper is an attempt to illustrate the use of flax fiber in hybrid composite systems as an alternative to E-glass in terms of fundamental frequency and cost. The design and optimization of laminated composites based on Differential Evolution (DE), Nelder Mead (NM) and Simulated Annealing (SA) algorithms is considered for stacking sequences. The task of optimization is to find the amount of high stiffness and less costly laminates by multi-objective optimization technique, optimizing the simple frequency and reduce the cost. The findings show that in terms of overall simple frequency and minimal cost, the proposed optimum graphite-

flax/epoxy inter-ply composite structure provides better than the graphite-glass/epoxy outcome (Savran and Aydin 2018).

1.2. Objectives

Literature survey is analyzed in detail, it is obvious that the design parameters include the strength of the panel, the properties of the material, weight, and rigidity. For a better configuration, it is thus essential to validate the ply thickness and stacking series. In the same way, in the configuration of the composite structures, the calculation of the buckling load potential of a laminated composite plate under in-plane compressive loads has serious implications. The buckling could give a premature structure failure. Accordingly, the purposes of the thesis can be listed as follows:

1. In order to find the best stacking sequences (fiber orientations with continuous fiber angles) of 48 and 64-layered graphite/epoxy, flax/epoxy, glass/epoxy, flax/polypropylene, glass/polyester, and carbon/epoxy laminated composites in different plate aspect ratios subjected to various compressive in-plane loads resisting buckling of any layers.
2. Determination and comparison of objective function (critical buckling load factor) values of optimized composite plates for each design cases.
3. To optimize critical buckling load factor by different stochastic optimization methods which are Differential Evolution, Simulated Annealing, and Nelder Mead.
4. To see the layer effect of the same materials used under the same loads, to compare the critical buckling load factor of 48 and 64-layered composite materials.
5. To obtain the best designs of 48-layered different composite plates subjected to specific compressive in-plane loading and comparison with the corresponding 64 layers plates in terms of buckling.

CHAPTER 2

COMPOSITE MATERIALS

2.1. Introduction

Composite materials can be defined as making a new material by combining two or more materials in macroscopic structure. The aim here is to improve the weaknesses of the materials used and to obtain a material that provides superior properties in the desired direction. For example, in the construction of a metal matrix composite, steel can be used as a reinforcement (fiber) material and aluminum as a matrix. Thus, it is benefited from the lightness of aluminum and the stronger structure of steel compared to aluminum.

Today, modern technology's need for materials with superior properties is increasing. Especially in addition to high strength, structures that require lightness are needed. Depending on the place of use, it is not possible to have such desired properties in the same material at the same time. Composite materials have been produced by combining superior properties to correct each other's weaknesses. In addition to the production of materials with the desired properties, it is also important to know their behavior against the damages that may occur during the working life and working.

2.2. Main Elements of Composite Materials

Composite materials have three main elements which are:
- Matrix element
- Reinforcement element
- Additives

2.2.1. Matrix Element

Matrix has three basic functions in composite materials. These are to hold the fibers together, distribute the load on the fibers and protect the fibers from environmental influences. An ideal matrix material should initially have a low viscosity structure and then easily transition to a solid form that can enclose the fibers in a robust and convenient

manner. Matrix material forms the continuous phase as a thermoset or thermoplastic polymer material. Mostly polyesters are used in the thermosets group. In addition, the use of vinyl ester/bisphenol, epoxy resin and phenolic resins is increasingly common. Polyamide and polypropylene are widely used in the thermoplastic group, besides, the use of polyethylene and polybutylene terephthalate, polyetheretherketone and polyethersulfone in hybrid form is also drawing attention.

Matrices show strong adhesion, high resistance to environmental and atmospheric conditions and high mechanical properties. The mechanical properties provided primarily by a matrix are high hardness and high durability values. A good material should be hard, but its performance should not decrease due to the behavior of a brittle material. Polymer-based matrices that meet these properties to a great extent are thermoset and thermoplastic matrices.

In addition to polymer-based matrices, metal and ceramic-derived materials are also used as matrix in composite materials. Metal matrices are too expensive to be used in large scale applications and very difficult to work with. Since ceramic matrices are highly fragile and do not have sufficient durability, their usage areas are limited to places used with high temperatures.

2.2.2. Reinforcement Element

The reinforcement element in the matrix material is the basic strength elements of the composite structure. In addition to their low density, fibers with high elasticity modulus and hardness are also resistant to chemical corrosion. Today, the most important reinforcement materials used in composite structures are continuous fibers. These fibers play an important role in the creation of modern composites. They are materials where aramid, carbon, graphite, boron, silicon carbide, alumina, glass and polyethylene are used in the form of short or long continuous fibers and whose matrix is about 60% by volume.

The physical form of the fibers used in composite materials is a very important factor on the properties of the new material created. Supplements basically come in 3 different forms; particles, discontinuous and continuous fibers. Although the particle is not generally spherical in shape, it is approximately equal in size in all directions. Examples of gravel, microballoons, and resin powder particle reinforcements are among

the examples. When one dimension of the reinforcement material is larger than the other, the fibers are mentioned.

Discontinuous fibers can range in size from a few millimeters to several centimeters. Most fibers do not exceed a few micrometers in diameter. For this reason, the fiber does not need to be too long for the transition from particle to fiber.

The main fiber types used in composite materials;

- Glass fiber
- Carbon (Graphite) fiber (PAN -polyacrylonitrile- and pitch origin)
- Aramid (Aromatic Polyamide) fiber (Trade name; Kevlar-DuPont)
- Boron fiber
- Silicon carbide fiber
- Alumina fiber

Although glass fiber is the most widely used and valid reinforcement material today, pure carbon fiber is generally used in advanced composite materials. Although carbon fiber is stronger and lighter than glass fiber, its production cost is higher. It is used in the skeletons of aircraft and sports vehicles as a substitute for metals. Stronger and more expensive than carbon fiber is boron fiber. It is a kevlar (aramid) polymer fiber that adds a very high level of strength and hardness to the composite material. Aramid is used in composite materials in products intended for lightness and reliable construction.

- Glass fibers

Glass fibers are manufactured in many types, from ordinary bottle glass to high purity quartz glass. Glass is an amorphous material and has a polymeric structure. Three

In dimensional molecular structure, a silicon atom is surrounded by four oxygen atoms. Silicium is a light non-metallic material, it is generally found in nature in the form of silica (SiO_2) with oxygen. For glass production, silica sand, together with its additives, is heated to around 1260 ° C in dry state and when it is left to cool, a hard structure is obtained.

Although the fibers lose 50% of their durability during the process, they are extremely strong. Glass fiber still has higher durability than aramid and carbon fibers. Fiber fabrics are generally produced with fibers of continuous glass fiber.

- Carbon fibers

Carbon is a crystalline material with a density of 2.268 gr / cm3. Carbon fibers are a widely used fiber group that developed later than glass fibers. Both carbon and graphite fibers are produced from the same base material.

The most important properties of carbon fibers are high strength and toughness values as well as low density. Carbon fibers are not affected by moisture and their creep resistance is very high. Its abrasion and fatigue strength is very good. Therefore, they are widely used in military and civil aircraft structures. Carbon fibers are used with various plastic matrices and most commonly epoxy resins. In addition, carbon fibers are used with metal matrices such as aluminum and magnesium.

- Aramid fibers

Aramid is the abbreviated name for aromatic polyamide. Polyamides are long chain polymers. In the molecular structure of aramid, six carbon atoms are bonded to each other by hydrogen atoms. There are two different types of aramid fibers. These are Kevlar 29 and Kevlar 49 developed by the Du Pont company. While the mechanical properties of aramid are very good in the direction of the fiber axis as in graphite fibers, it is very poor in the vertical direction to the fibers. Aramid fibers have the characteristics of low weight, high tensile strength and low cost. High impact resistance,

Its brittleness is half that of graphite. Therefore, it can be shaped easily. It is resistant to natural chemicals but is affected by acids and alkalis.

The impact strength of Kevlar49 / epoxy composites is seven times better than graphite epoxy composites and four times better than boron / epoxy composites. In aircraft structures, due to their low compressive strength, they are used as hybrid composite together with carbon fibers on control surfaces. Aramid fibers do not have electrical conductivity. In addition to poor compression strength, the moisture absorption properties of Kevlar epoxy composites are poor.

- Boron fibers

Boron fibers are actually composite in themselves. They are manufactured by coating boron on a thin filament called core. The core is usually tungsten. Carbon core can also be used, but this is a new application. Boron fibers are resistant to high temperatures by coating them with silicon carbide (SiC) or boron carbide (B4C). Especially with boron carbide coating, the tensile strength can be increased significantly.

- Silicon carbide fibers

Like boron, they are obtained by coating silicon carbide on a tungsten core. They are produced in diameters of 0.1 mm to 0.14 mm. High temperature properties are better than boron fibers. Silicon carbide fiber loses only 30% of its strength at 1370 ° C. For boron fiber, this temperature is 640 ° C. These fibers are generally used with titanium

matrix. They are used with titanium, aluminum and vanadium alloy matrix in jet engine parts. However, silicon carbide fibers have higher density than boron fibers.

- Alumina fibers

Alumina is aluminum oxide (A12O3). The alumina in fiber form is obtained by coating the 0.02 mm diameter alumina filament with silicon dioxide (SiO2).

The tensile strength of alumina fibers is not high enough, but their compression strength is high.

2.2.3. Additives

Fillers, chemicals and other additives are added to the matrix in order to improve its properties according to its properties.

2.3. Classification of Composite Materials

Although it is not possible to draw clear boundaries in the grouping of composites that can use a large number of different materials in their structures, it is possible to make a classification according to the form of the materials in the structure in Figure 2.1.

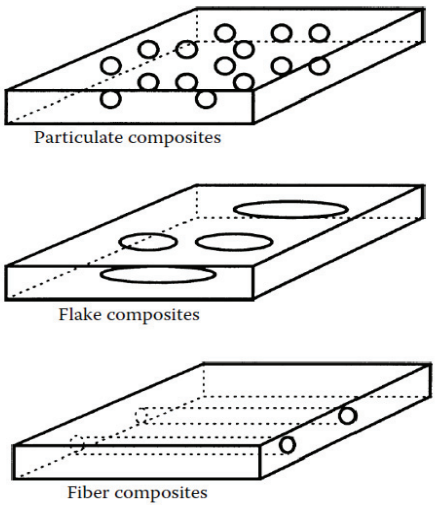

Figure 2.1. Types of composites based on reinforcement shape
(Source: Aboudi, Arnold, and Bednarcyk 2013)

2.3.1. Fiber Composites

When most of the materials used in engineering are produced in the form of fibers, their strength and stiffness can be much higher than their mass values. It is obtained by the addition of high efficiency fibers that provide an increase in many properties. The tensile strength of carbon fibers is 50 times higher than the mass graphite, and its stiffness is three times higher.

There are different types of fiber composites, four types as shown in Figure 2.2. These are:

- Unidirectional reinforced continuous fiber composite
- Composites reinforced with fibers in knitted form
- Randomly oriented discontinuous fiber composite
- Oriented discontinuous fiber composite

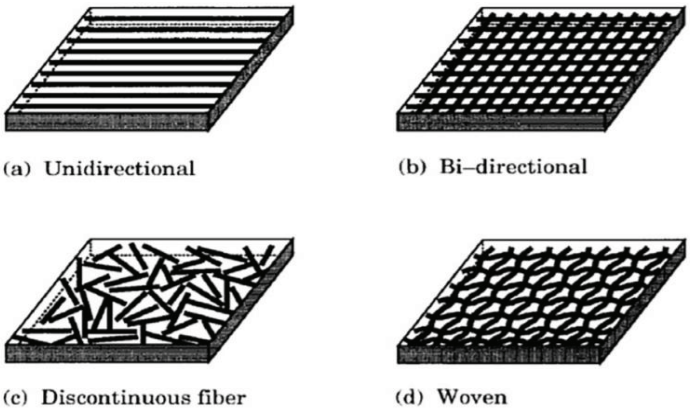

Figure 2.2. Different types of fiber composites
(Source: Tawfik et al. 2017)

The most important factors affecting the engineering performance of fiber-matrix composites are the shape, length, orientation of the fibers, the mechanical properties of the matrix and the fiber-matrix interface properties. The fibers may be circular as well as more rarely rectangular, hexagonal, polygonal and hollow circular cross-section. Although these sections have some positive features, circular sections provide superiority with their cost and ease of use. Although it is generally easier to work with continuous fibers, design freedom is much more limited than with discontinuous ones. Although

continuous fibers show better orientation than discontinuous fibers, the use of discontinuous fibers gives more practical results (Ünal 2005).

This composite type is formed by the presence of fine fibers in the matrix structure. The placement of the fibers in the matrix is an important factor affecting the strength of the composite structure. By placing long fibers in the matrix parallel to each other, high strength is achieved in the direction of the fibers, while a very low strength is obtained in the vertical direction of the fibers. It is possible to create an isotropic structure with short fibers homogeneously distributed in the matrix structure, while two-dimensional fiber reinforcements provide equal strength in both directions.

The strength of the fibers is very important in terms of the strength of the composite structure. Also, as the length / diameter ratio of the fibers increases, the amount of load transmitted by the matrix to the fibers increases. The fact that the fiber structure is faultless is also very important in terms of strength.

Another important factor in the strength of the composite structure is the structure of the bond between the fiber matrix. If there are gaps in the matrix structure, contact with the fibers will be reduced. Moisture absorption is also a negative feature that disrupts the bond between fiber and matrix.

2.3.2. Flake Composites

Flake composites consist of flat reinforcements of matrices. Typical flake materials are glass, mica, aluminum and silver. Flake composites provide advantages such as high out-of-plane flexural modulus, higher strength and lower cost. However, stamps cannot be easily manipulated and can only be used for a limited number of uses (Claassen 2009).

2.3.3. Particulate Composites

It is produced by shaping with the addition of small granule filler that increases rigidity and strength. They are materials formed by matrix phase of one or two dimensional macroscopic particles or very small microscopic particles, which are considered to be zero-dimensional. Macroscopic or microscopic sized particles affect the

composite material properties differently. Microscopic size particulate composites can be seen in Figure 2.3. as a few examples.

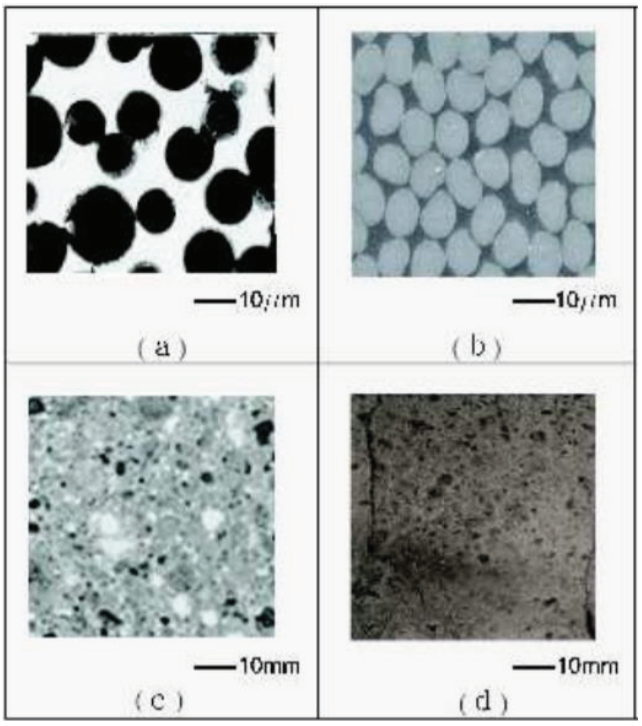

Figure 2.3. Examples of particulate composites: ceramic/metal matrix composites (a,b); Roman concrete (c), tuffaceous rock (d) (Source: Sadowski et al. 2014)

They are obtained by the presence of another material in the form of particles in a matrix material. They are isotropic structures. The strength of the structure depends on the hardness of the particles. The most common type are metal particles contained in a plastic matrix. Metal particles provide thermal and electrical conductivity. Structures containing ceramic particles in a metal matrix have high hardness and high temperature resistance. They are preferred in the production of aircraft engine parts (Ünal 2005).

2.3.4. Layered Composites

It is possible to produce layered composites with very different combinations. It consists of a combination of at least two layers with different properties. It is possible to improve the corrosion property by coating metals or plastics with higher resistance on metals with poor corrosion resistance, and to improve hardness and wear resistance by combining soft metals with hard materials. An example of a multi-layer composite

structure is the Figure 2.4. In this figure, all layers are of equal thickness and symmetrical order.

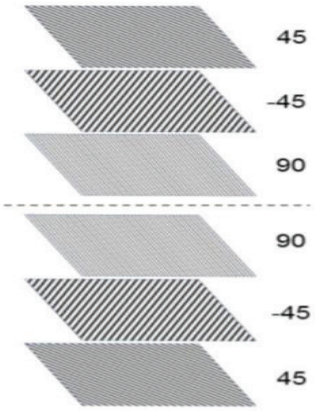

Figure 2.4. Multi-Layered composite material
(Source: Andhini 2017)

Layered composite structure is the oldest and most widely used type. Very high strength values are obtained with the combination of layers with different fiber orientations. They are heat and moisture resistant structures. They are preferred materials due to their lightness and strength compared to metals. Continuous fiber reinforced layered composites have a very common use in aircraft structures, as a surface coating material in the wing and tail group.

In addition, sandwich structures, which are widely used in aircraft structures, are examples of laminated composite materials. Sandwich structures are obtained by adhering resistant boards to the lower and upper surfaces of a low density core material that does not carry loads and has only insulation properties.(Charkviani, Pavlov, and Pavlova 2017)

2.3.5. Mixed (Hybrid) Composites

It is possible to have two or more types of fibers in the same composite structure. These types of composites are called hybrid composites. This area is suitable for the development of new types of composites. As an example, Kevlar is a cheap and tough fiber but has a low compression force. Graphite, on the other hand, is an expensive fiber with low toughness but good compression. The toughness of the hybrid composite, which is obtained by combining these two fibers in the composite structure, is better than

graphite composite, its cost is lower, and its compression strength is higher than the kevlar fiber composite. At the same time, the configurations of hybrid composites can be of different types, as shown in Figure 2.5.

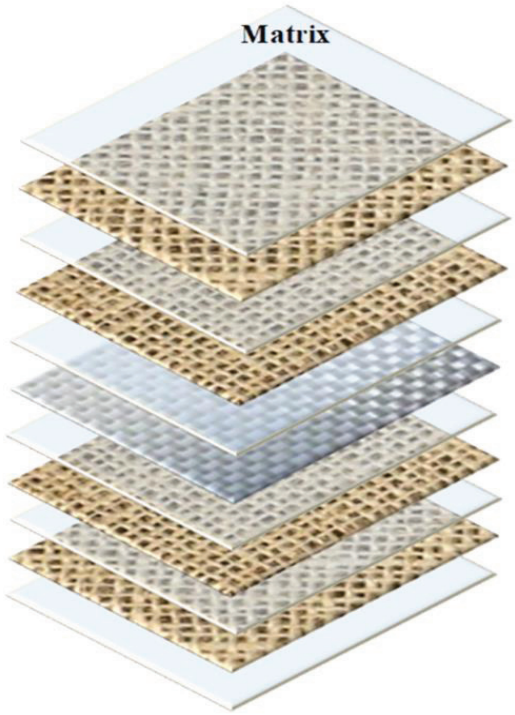

Figure 2.5. Configurations of hybrid composite laminates
(Source: Fontes et al. 2019)

Different types of hybrid composites can be grouped as follows;

1. They contain two or more layers in the matrix. Each layer contains reinforcements in a specific direction, and a specific type of fiber is used in each layer. The layers are placed as desired according to the purpose.

2. Two or more fibers are placed in the same layer as a mixture and the layers are combined as desired to obtain a hybrid composite.

3. Superhybrids containing different composite structures such as resin matrix layers and metal matrix layers can be obtained. In super hybrids layers are combined with an adhesive material (Ünal 2005).

2.3.6. Lamella Based Composites

It is produced by adding filler material in a large length / diameter ratio with high load carrying ability. The concentration of the flakes in the matrix may be low or high

enough to allow them to come into contact with each other. Tight packaging can be obtained with planar washers. The cost of the flake-based system is a little more, but its strength properties are good. The alignment of lamella composites can take place in different variations depending on the nature of the area to be used in Figure 2.6.

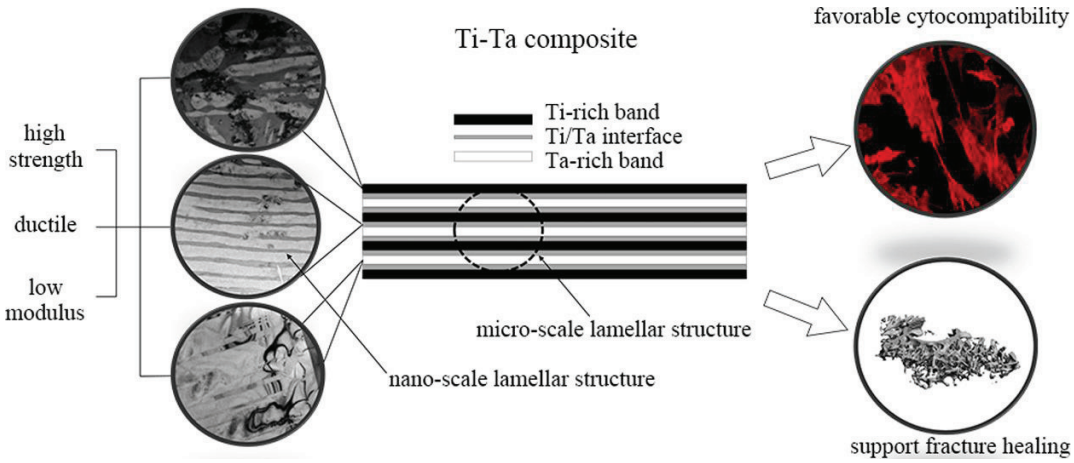

Figure 2.6. Micro-scale and nano-scale example of lamella composite
(Source: Huang et al. 2021)

2.3.7. Filler Composites

They are materials formed by filling or impregnating a three dimensional continuous matrix material with 3 dimensional filler. Metallic organic or ceramic-based fillers may include smooth combs, cells, or porous structures that resemble sponges. In order to have optimum properties, components that are insoluble and do not react chemically should be selected. These types of composites are also known as sandwich composites (Dahal et al. 2019).

2.4. Composite Materials Used in the Thesis

The materials used in the thesis have been carefully selected as they have different properties. Especially in sectors such as aircraft, aviation and automotive sectors where material lightness and elastic properties are important, these materials are used or these materials are at the stage of use. Short features of these materials are given here as:

Graphite/Epoxy is a member of conductive polymer composites. Especially in the lattice and platform structures used in space and satellites, if the air temperature is approximately -160°C to 90°C degrees, if monolithic materials cannot meet this requirement, graphite/epoxy material can be used 17ort he17 purpose. Its advantages are high specific strength and modulus, low thermal expansion coefficient and high fatigue strength. The disadvantages are high cost, low impact resistance and high electrical conductivity.

Glass/Epoxy, glass fiber is the most common type of fiber used in Polymer Matrix Composites (PMC). The advantages are high strength and chemical resistance, low cost and good insulation properties. The drawbacks are low elastic modulus, high specific gravity, friction sensitivity and low fatigue strength.

Carbon/Epoxy, carbon reinforced composites are materials that were first developed for use in rockets and fighter jets used in space research, and found as a result of researches where the presence of a light material that provides the desired structural, mechanical and thermal properties is at the forefront, and the cost is second. Especially the use of Carbon/epoxy is generally used in areas where cost is not important, more strength is required.

Flax/Epoxy, detailed studies are carried out on the use of flax/epoxy as an alternative to traditional derivatives of glass fiber/epoxy in terms of vibration damping, price-performance index, non-flammability and high adhesion capability, and impact behavior. Its use has increased, especially in hybrid structures.

Glass/Polyester is formed by combining high mechanical strength fiberglass and filling materials. It can be obtained using very simple techniques. However, the main principle is to wet the glass fiber with polyester. Here, it is polymerized through a polyesterchemical reaction and converted into a hard, insoluble substance. It is seen as the material of the future in many sectors. It will replace steel and its derivatives very soon.

Flax/PP, the use of natural fibers as reinforcement in thermoplastics presents an interesting alternative 17ort he production of low cost and ecologically friendly composites such as flax. One of the advantages of using fax/pp is their low specific weight, resulting in higher specific strength and stiffness when compared to glass-reinforced composites. Natural fibers also present safer handling and working conditions.

CHAPTER 3

MECHANICS OF COMPOSITES

3.1. Introduction

Composites are especially increasingly used materials today. Compared to other materials, it has become more preferred especially in the aviation industry due to its advantages such as light weight, high yield limits, and less corrosion problem. Although they are the preferred materials of most engineers, especially in industry, they are expensive to manufacture, they are affected by moisture and air particles, and drilling and cutting processes cause fibers to open.

Considering the mechanical advantage of composite materials, it is seen that specific strength and specific modulus values are high. For example, a unidirectional graphite/epoxy composite may have the same strength as steel but has a specific strength three times higher than steel. Figure 3.1 shows the comparison of composites and fibers with the other traditional materials in terms of specific strength on yearly basis.

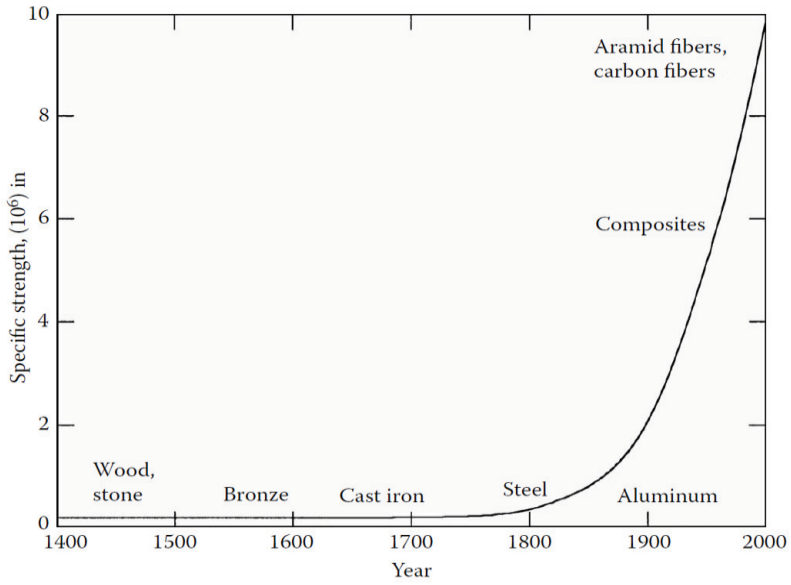

Figure 3.1. Specific strength as a function of time of use of materials

(Source: Kaw, 2006)

Specific strength values to be considered in Figure 3.1. are inches. Specific strength and specific modulus can be defined as follows.

$$\text{Specific modulus} = \frac{E}{\rho.g} \quad , \quad \text{Specific Strength} = \frac{\sigma_{ult}}{\rho.g} \tag{3.1}$$

Here, E = Young's modulus of elasticity of the material of the rod, ρ = Density of the material of the rod, g = Gravitational acceleration (32.2 ft/s^2, 9.81 m/s^2)

3.2. Classical Lamination Theory

Laminated plate theory or classical lamination theory is the basic design tool used to evaluate different laminates when experimental data are not available. Laminated plate theory is used to estimate overall performance characteristics for a laminate by evaluating the properties and orientations of each ply within a predetermined stacking order. The laminated plate theory is based on deforming assumptions under plane stress conditions and that the individual strains of the laminate are compatible with the neighboring layer strains. Before theory is required, the mechanical properties of a unidirectional composite are required, which are best derived from mechanical tests. If there is no mechanical test data, approximate values given in the literature can be used. Laminated Sheet Theory can also be used to evaluate the stresses caused by changes in temperature and humidity. This theory includes the in-plane stresses and strains for each laminate. In addition, the failure criteria for each lamina can be calculated.

The following assumptions are used in the application of this theory:

1- Nonhomogeneous and orthotropic are each lamina of the laminated composite.
2- The laminate is thin, and the composite plate 's edge dimensions are much greater than its size. In the laminate plane, the loadings are added, and the laminate is in a state of plane stress.
3- Comparison with the laminate width, all displacements are minimal, and they are constant in the laminate.
4- Directions are linear functions of z in the plane displacements of x and y.
5- There are insignificant transverse shear strains γ_{XZ} and γ_{YZ}.
6- Relations between stress-strain and strain-displacement are linear.

7- There is a negligible transverse normal strain of ε_Z.

Figure 3.2. shows the thin laminated composite structure subjected to mechanical in-plane loading (N_x, N_y) considered in this thesis. The cartesian scheme of coordinates x, y, and z determines the layered material 's global coordinates. 1, 2, 3 denote a layer wise main material coordinate scheme, and the orientation of the fiber is aligned at an angle to the x axis. Figure 3.3. shows a representation of a symmetrical laminate. Here the thickness of the letter h; k represents the number of layers.

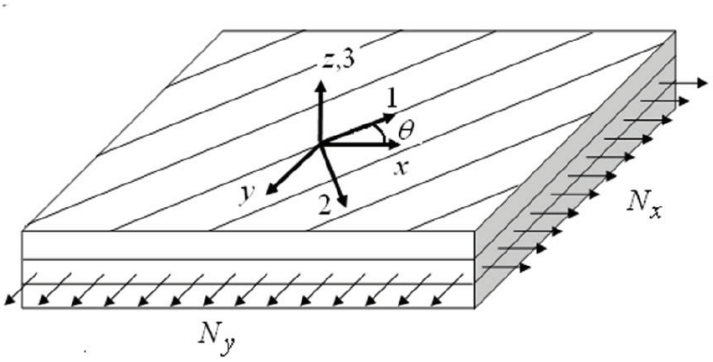

Figure 3.2. A thin fiber-reinforced laminated composite subjected to in-plane loading (Source: Kaw, 2006)

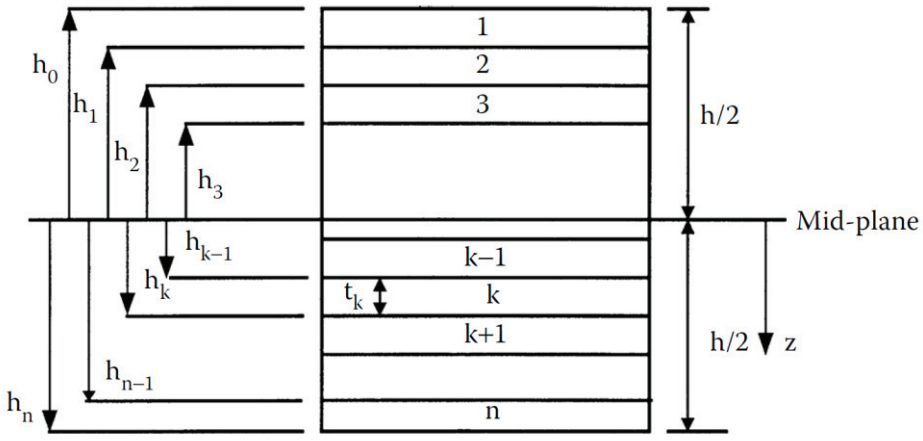

Figure 3.3. Schematic representation of a symmetric laminate (Source: Kaw, 2006)

Composite materials in the form of thin laminates loaded onto the laminate plane are used in most structural applications. Composite laminates can thus be assumed to be under a plane stress condition, with all stress components being zero in the out-of-plane direction (direction 3). For the k-th layer of a composite plate, the stress-strain relation based on the classical lamination theory can be written in the following form:

$$\begin{bmatrix} \sigma_x \\ \sigma_y \\ \sigma_{xy} \end{bmatrix}_k = \begin{bmatrix} \overline{Q}_{11} & \overline{Q}_{12} & \overline{Q}_{16} \\ \overline{Q}_{12} & \overline{Q}_{22} & \overline{Q}_{26} \\ \overline{Q}_{16} & \overline{Q}_{26} & \overline{Q}_{66} \end{bmatrix}_k \left(\begin{bmatrix} \varepsilon_x^o \\ \varepsilon_y^o \\ \varepsilon_{xy}^o \end{bmatrix} + z \begin{bmatrix} \kappa_x \\ \kappa_y \\ \kappa_{xy} \end{bmatrix} \right)_k \tag{3.1}$$

where the components of the transformed reduced stiffness matrix are $[\overline{Q}_{ij}]_k$, $[\varepsilon^0]$ are the mid-plane strains, respectively, $[\kappa]$ are curvatures.

The transformed reduced stiffness matrix elements $[\overline{Q}_{ij}]$ given in Eq. (3.1) can be defined as follows

$$\overline{Q}_{11} = Q_{11}c^4 + Q_{22}s^4 + 2(Q_{12} + 2Q_{66})s^2c^2 \tag{3.2}$$

$$\overline{Q}_{12} = (Q_{11} + Q_{22} - 4Q_{66})s^2c^2 + Q_{12}(c^4 + s^4) \tag{3.3}$$

$$\overline{Q}_{22} = Q_{11}s^4 + Q_{22}c^4 + 2(Q_{12} + 2Q_{66})s^2c^2 \tag{3.4}$$

$$\overline{Q}_{16} = (Q_{11} - Q_{12} - 2Q_{66})sc^3 - (Q_{22} - Q_{12} - 2Q_{66})s^3c \tag{3.5}$$

$$\overline{Q}_{26} = (Q_{11} - Q_{12} - 2Q_{66})cs^3 - (Q_{22} - Q_{12} - 2Q_{66})sc^3 \tag{3.6}$$

$$\overline{Q}_{66} = (Q_{11} + Q_{22} - 2Q_{12} - 2Q_{66})s^2c^2 + Q_{66}(c^4 + s^4) \tag{3.7}$$

where stiffness matrix quantities $[Q_{ij}]$ are

$$Q_{11} = \frac{E_1}{1 - \nu_{21}\nu_{12}} \tag{3.8}$$

$$Q_{12} = \frac{\nu_{12}E_2}{1 - \nu_{21}\nu_{12}} \tag{3.9}$$

$$Q_{22} = \frac{E_2}{1 - \nu_{21}\nu_{12}} \tag{3.10}$$

$$Q_{66} = G_{12} \tag{3.11}$$

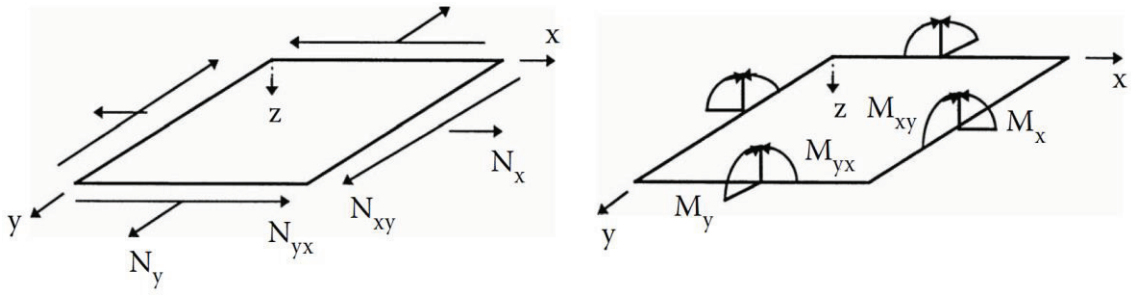

Figure 3.4. Resultant Forces and Resultant Moments on a composite laminate
(Source: Kaw, 2006)

Applied normal force resultants N_x, N_y, shear force resultant N_{xy} (per unit width), and moment resultants M_x, M_y, and M_{xy} on a laminate (Fig. 3.4.) have the following relationships:

$$\begin{bmatrix} N_x \\ N_y \\ N_{xy} \end{bmatrix} = \begin{bmatrix} A_{11} & A_{12} & A_{16} \\ A_{12} & A_{22} & A_{26} \\ A_{16} & A_{26} & A_{66} \end{bmatrix} \begin{bmatrix} \varepsilon_x^0 \\ \varepsilon_y^0 \\ \gamma_{xy}^0 \end{bmatrix} + \begin{bmatrix} B_{11} & B_{12} & B_{16} \\ B_{12} & B_{22} & B_{26} \\ B_{16} & B_{26} & B_{66} \end{bmatrix} \begin{bmatrix} \kappa_x \\ \kappa_y \\ \kappa_{xy} \end{bmatrix} \tag{3.12}$$

$$\begin{bmatrix} M_x \\ M_y \\ M_{xy} \end{bmatrix} = \begin{bmatrix} B_{11} & B_{12} & B_{16} \\ B_{12} & B_{22} & B_{26} \\ B_{16} & B_{26} & B_{66} \end{bmatrix} \begin{bmatrix} \varepsilon_x^0 \\ \varepsilon_y^0 \\ \gamma_{xy}^0 \end{bmatrix} + \begin{bmatrix} D_{11} & D_{12} & D_{16} \\ D_{12} & D_{22} & D_{26} \\ D_{16} & D_{26} & D_{66} \end{bmatrix} \begin{bmatrix} \kappa_x \\ \kappa_y \\ \kappa_{xy} \end{bmatrix}$$

(3.13)

The matrices [*A*], [*B*], and [*D*] stated in the following Eqs. (3.14 - 3.16) can be defined as:

$$A_{ij} = \sum_{k=1}^{n} [(\overline{Q}_{ij})]_k (h_k - h_{k-1}), \quad i, j = 1,2,6 \tag{3.14}$$

$$B_{ij} = \frac{1}{2} \sum_{k=1}^{n} [(\overline{Q}_{ij})]_k (h_k^2 - h_{k-1}^2), \quad i, j = 1,2,6 \tag{3.15}$$

$$D_{ij} = \frac{1}{3} \sum_{k=1}^{n} [(\overline{Q}_{ij})]_k (h_k^3 - h_{k-1}^3), \quad i, j = 1,2,6 \tag{3.16}$$

The [A], [B], and [D] matrices are respectively called the extensional, coupling, and bending stiffness matrices. Six simultaneous linear equations and six unknowns are given by combining Eq. (3.12) and Eq. (3.13) as:

$$\begin{bmatrix} N_x \\ N_y \\ N_{xy} \\ M_x \\ M_y \\ M_{xy} \end{bmatrix} = \begin{bmatrix} A_{11} & A_{12} & A_{16} & B_{11} & B_{12} & B_{16} \\ A_{12} & A_{22} & A_{26} & B_{12} & B_{22} & B_{26} \\ A_{16} & A_{26} & A_{66} & B_{16} & B_{26} & B_{66} \\ B_{11} & B_{12} & B_{16} & D_{11} & D_{12} & D_{16} \\ B_{12} & B_{22} & B_{26} & D_{12} & D_{22} & D_{26} \\ B_{16} & B_{26} & B_{66} & D_{16} & D_{26} & D_{66} \end{bmatrix} \begin{bmatrix} \varepsilon_x^0 \\ \varepsilon_y^0 \\ \gamma_{xy}^0 \\ \kappa_x \\ \kappa_y \\ \kappa_{xy} \end{bmatrix} \tag{3.17}$$

The extensional stiffness matrix [A] applies the resultant in-plane forces to the in-plane strains, and the bending stiffness matrix [D] applies the resultant moment of bending to curvature of the plates. The coupling stiffness matrix [B] couples the terms of force and moment to the mid-plane strains and mid-plane curvatures (Kaw, 2006).

Stresses and stress expressions based on the classical theory of lamination can

now be represented by local coordinate system (1, 2). It is possible to define the relation between local and global stresses in an angled lamina in the following form

$$\begin{bmatrix} \sigma_1 \\ \sigma_2 \\ \sigma_{12} \end{bmatrix} = [T] \begin{bmatrix} \sigma_x \\ \sigma_y \\ \sigma_{xy} \end{bmatrix} \tag{3.18}$$

Likewise, the local and global strains are associated as follows

$$\begin{bmatrix} \varepsilon_1 \\ \varepsilon_2 \\ \varepsilon_{12} \end{bmatrix} = [R][T][R]^{-1} \begin{bmatrix} \varepsilon_x \\ \varepsilon_y \\ \varepsilon_{xy} \end{bmatrix} \tag{3.19}$$

where

$$[R] = \begin{bmatrix} 1 & 0 & 0 \\ 0 & 1 & 0 \\ 0 & 0 & 2 \end{bmatrix} \tag{3.20}$$

and $[T]$ transform matrix,

$$[T] = \begin{bmatrix} c^2 & s^2 & 2sc \\ s^2 & c^2 & -2sc \\ -sc & sc & c^2 - s^2 \end{bmatrix} \tag{3.21}$$

where

$$c = \cos\theta, \quad s = \sin\theta$$

3.3. Buckling Theory of Composite Plates

Fiber-reinforced composites have gained further interest from engineers, scientists, and manufacturers due to their outstanding stiffness and weight characteristics. The composite laminate plates are typically exposed to compression loads during service that can cause buckling if overloaded. Their buckling behaviors are also essential variables in the safe and stable construction of such systems. (Baba 2007)

The governing differential equation for the buckling behavior of the plate, taking into account the classical plate theory, assuming that the composite plate under consideration (Figure 3.1) is loaded by λN_x, λN_y and λN_{xy} in-plane compressive loads, where λ is a scalar amplitude parameter and clearly provided on four sides.

$$D_{11}\frac{\partial^4 w}{\partial x^4}+2\left(D_{12}+2D_{66}\right)\frac{\partial^4 w}{\partial x^2\partial y^2}+D_{22}\frac{\partial^4 w}{\partial y^4}=\lambda\left(N_x\frac{\partial^2 w}{\partial x^2}+N_y\frac{\partial^2 w}{\partial y^2}+N_{xy}\frac{\partial^2 w}{\partial x\partial y}\right) \quad (3.22)$$

where D_{11}, D_{12}, D_{22}, D_{66} are the terms of bending stiffnesses, w is the vertical displacement given by

$$w(x,y)=\sum_m\sum_n A_{mn}\sin\frac{m\pi x}{a}\sin\frac{n\pi y}{b} \quad (3.23)$$

With the substitution of Eq. (3.23) to Eq. (3.22), buckling load factor expression can be obtained as in the following form

$$\lambda_b=\frac{\pi^2\left[D_{11}\left(\frac{m}{a}\right)^4+2\left(D_{12}+2D_{66}\right)\left(\frac{m}{a}\right)^2\left(\frac{n}{b}\right)^2+D_{22}\left(\frac{n}{b}\right)^4\right]}{N_x\left(\frac{m}{a}\right)^2+N_y\left(\frac{n}{b}\right)^2+N_{xy}\left(\frac{m}{a}\right)\left(\frac{n}{b}\right)} \quad (3.24)$$

A noteworthy fact is that in Eq. (3.22) and Eq. (3.23), D_{16} and D_{26} do not occur because they are zero for a clearly orthotropic laminate and are small for a symmetric laminate with a number of laminas in sequence of ± ply angles relative to the other D_{ij}'s.

As the magnitude parameter exceeds a critical value of λ_b, the laminate buckles into m and n half-waves in the x and y directions respectively. The critical buckling load factor λ_{cb} restricts the overall load that the laminate can bear without buckling and under acceptable m and n values is the smallest value of λ_b.The essential values of m and n are minimal whether the plate has a very high aspect ratio or excessive ratios of D_{ij}'s.

If the laminated composite is not especially orthotropic, the effects of the D_{16} and D_{26}, bending and twisting terms, would be ignored if the non-dimensional parameters have the following conditions:

$$\gamma \leq 0.2, \delta \leq 0.23 \tag{3.25}$$

where

$$\gamma = D_{16}(D_{11}^3 D_{22})^{-1/4} \tag{3.26}$$

$$\delta = D_{26}(D_{22}^3 D_{11})^{-1/4} \tag{3.27}$$

In order to prevent any unexpected failure, the critical buckling load factor λ_{cb}varies with the plate aspect ratio, loading ratio and material, and should be greater than one.

$$\lambda_{cb} = min\, \lambda_b\,(m,n) \tag{3.28}$$

In the thesis study, the optimization problem we have considered is to find the best configurations of composite plates with the highest critical buckling load factors, λ_{cb}. To result in a rough guesstimate of buckling load capacity, the values of m and n are taken to be 1 or 2. In the thesis study, then, the smallest of $\lambda_b(1,1)$, $\lambda_b(1,2)$, $\lambda_b(2,1)$, $\lambda_b(2,2)$ yields λ_{cb} (Erdal and Sonmez 2005).

Critical buckling loads can be calculated by means:

$N_{x,cr} = \lambda_{cb} N_x$ and $N_{y,cr} = \lambda_{cb} N_y$ expressions after the critical buckling load factor has been obtained.

CHAPTER 4

OPTIMIZATION

4.1. Introduction

From engineering design to capital markets, from our everyday lives to preparing our vacations, and from computer science to manufacturing applications, optimization is widely used. People either tend to optimize something or to minimize it. In reality, we are always looking for the right solutions to any issue we face, but we are not always able to find those solutions.

Optimization is a set of mathematical processes aimed at seeking optimal case design through minimizing or optimizing specified single or multiple goals with the fulfillment of provided limitations. For engineering issues such as failure, weight, cost, temperature, buckling, vibration, etc., optimization is also discussed. In these problems, to achieve optimal solutions, minimization or maximization of objective or multi-objectives is applied.

There is only one function to be reduced or maximized with single or more constraints and connections from the first form of optimization. Optimization of only one target may interfere with other parameters in certain situations. Therefore, given multi-objective design, optimization issues with multi-bounds should be controlled. Since the optimal solution for each objective cannot be achieved, Pareto's optimal solutions are calculated using a multi-objective strategy.

Anisotropic materials are such as laminated composite structures, making them more complex and impossible to analytically construct since they consist of strongly nonlinear functions. In this case, conventional optimization methods from the requirements that may require optimization of these materials may be inadequate. For the optimization problems of composites, stochastic search algorithms are therefore more fitting. Often, stochastic optimization algorithms are used by Differential Evolution (DE), Nelder Mead (NM), Genetic Algorithm (GA), Simulated Annealing (SA).

In this study, the design and optimization of composite materials with different properties has been made using MATHEMATICA software, which offers a suitable platform for optimization problems. The program consists of four stochastic optimization algorithms in the database, namely DE, NM, RS and SA, which are widely used by researchers in the design and optimization situations of composites. The problems in the study were solved using DE, SA, and NM. In this way, the comparison of three different stochastic approaches is examined.

4.2. Single-Objective Optimization

To minimize or maximize, single-objective optimization is applied to single objective functions. The goal of a single-objective optimization problem is to find the best solution for a particular criterion or metric, such as time or efficiency of execution or a mixture of this metric with energy consumption or metrics of power dissipation. The limits of design variables, restrictions and limits of limitations are included in this optimization approach. The issues solved by the approach to single-purpose optimization are expressed as follows.

The minimization	$f(x)$
Subject to	$g_i \leq 0$
	$h_n = 0$
	$x_1, x_2, \ldots x_m$

where f(x) is the objective function, g_i is the inequality constraints h_n is the equality constraints and x_1, x_2 etc are the design variables. The i, n and m are integers.

4.3. Multi-Objective Optimization

Multi-objective optimization issues include two or more competing optimization objectives, meaning that progress to one goal comes at the cost of another goal. Multi-objective optimization is a field of decision-making of multiple parameters that tackles issues of mathematical optimization involving more than one objective function that can

be optimized simultaneously. For a non-trivial multi-objective optimization problem, there is no single solution that optimizes each objective simultaneously. The objective functions are said to be contradictory in that case, and there are a (possibly infinite) number of optimal solutions from Pareto.

The minimization $\{f_1(x), f_2(x), \ldots . f_k(x)\}$

Subject to $g_i \leq 0$

$h_n = 0$

$\{x_1, x_2, \ldots x_m\}$

where $f_1(x), f_2(x)$ etc. are the objective function, g_i is the inequality constraints h_n is the equality constraints and x_1, x_2 etc are the design variables. The i, n, and m are integers.

4.4. Stochastic Optimization Algorithms

Methods of stochastic optimization are methods of optimization that create and use random variables. In the formulation of the optimization problem itself which requires random objective functions or variable constraints, random variables appear for stochastic problems. Methods of stochastic optimization also provide strategies of random iterations. In order to solve stochastic problems, some stochastic optimization approaches use random iterates, incorporating all definitions of stochastic optimization. Problems of composite structures consist of highly discrete search spaces; traditional optimization methods fail to meet obtaining optimum results. In these situations, non-traditional search algorithms such as DE, NM, SA, and GA are preferred to find optimum solutions. Rao (2009) expressed a detailed discussion of different optimization methods for general applications while Gurdal et al. (1999), studied them for the usage in composites. In this study, DE and NM are used to obtain optimum stacking sequence design at desired burst pressure of composite pressure vessels. In following sections, procedures for these algorithms are explained in step wise formation.

4.4.1. Nelder-Mead (NM)

A conventional local search technique is the Nelder-Mead algorithm. It was developed primarily for an unconstrained optimization problem by Nelder and Mead (1965). The Nelder-Mead solution has not been planned for restricted issues. Even though Nelder-Mead is not a global optimization algorithm, in practical usage, it is very useful for issues that do not have too much local minimum. The flowchart of the Nelder-Mead algorithm is shown in Figure 4.1.

4.4.2 Random Search (RS)

Random search is a family of numerical optimization methods that do not require the gradient of the problem to be optimized, and random search can hence be used on functions that are not continuous or differentiable. The Random Search method is a stochastic-based algorithm that is quite different from the deterministic methods of Branch and Bound, Interval Analysis and Tunneling.

The random search method is based on solving equations by giving random numbers and finding the most approximate solution. The benefit of the RS approach is that complex problems are relatively easy to implement. In general, because of the rapid outcomes of poorly organized global optimization problems, RS algorithms are considered to be strong" and perform well. The flowchart of the Random Search algorithm is shown in Figure 4.2.

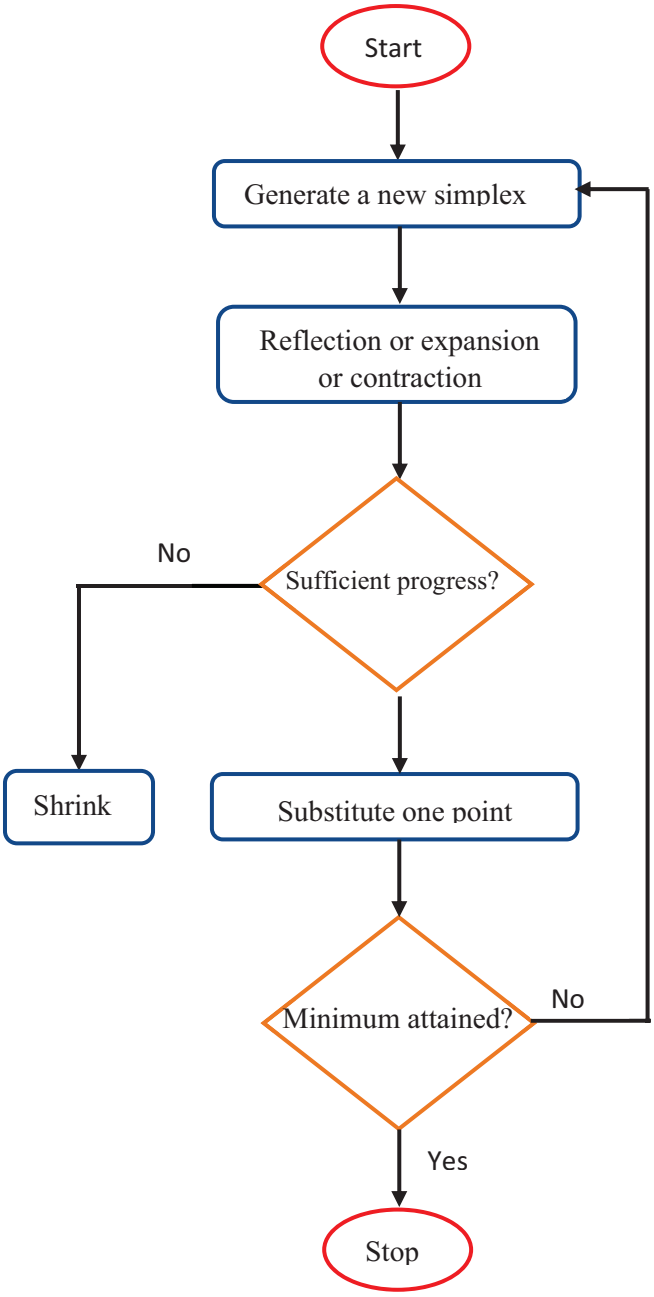

Figure 4.1. The flowchart of Nelder-Mead Optimization Algorithm

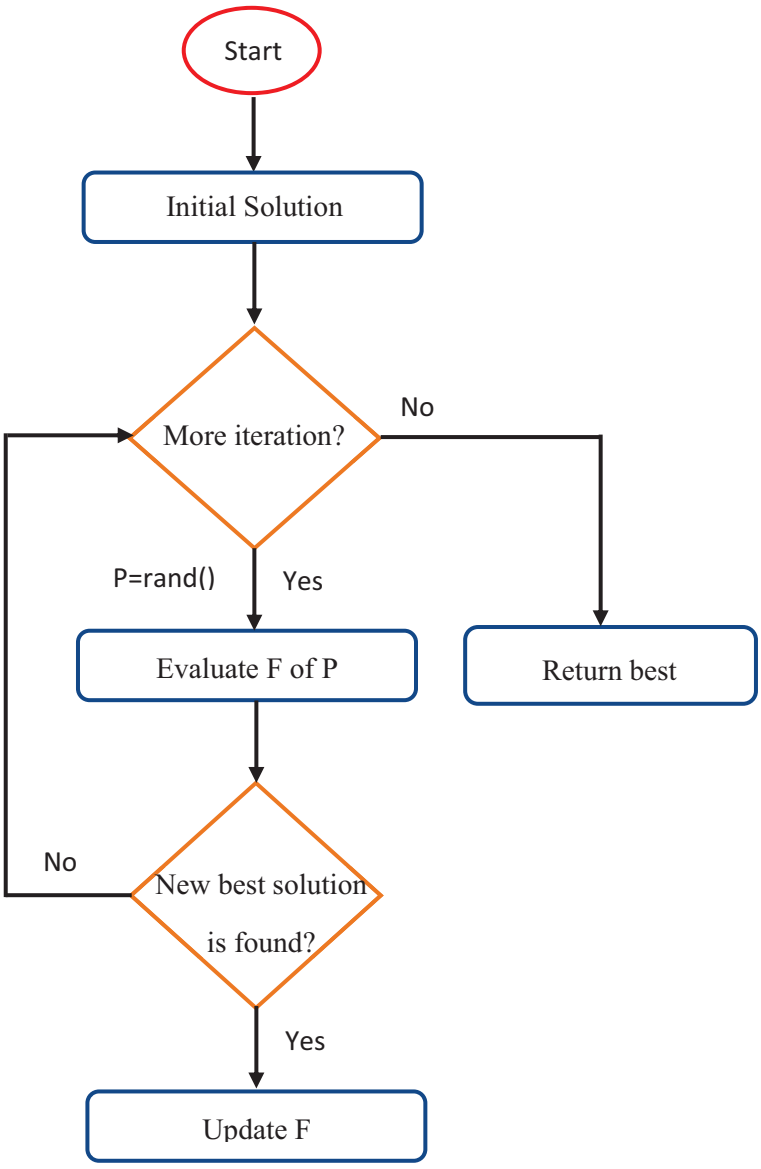

Figure 4.2. The flowchart of Random Search optimization algorithm

4.4.3. Differential Evolution (DE)

Differential evolution (DE) is a type of evolutionary algorithm developed by Rainer Storn and Kenneth Price for optimization problems over a continuous domain. (Plagianakos, Magoulas, and Vrahatis, n.d.)

Each variable's value in DE is expressed also by actual number. Simple structure, simple to use, quick and robust are the benefits of DE. DE is one of the best algorithm style to solve problem with the real-valued variables. In a range of scientific and engineering applications, DE has been used to provide solutions to almost all issues that can not be solved without resorting to expert knowledge or sophisticated design algorithms. The flowchart of the Differential Evolution algorithm is shown in Figure 4.3.

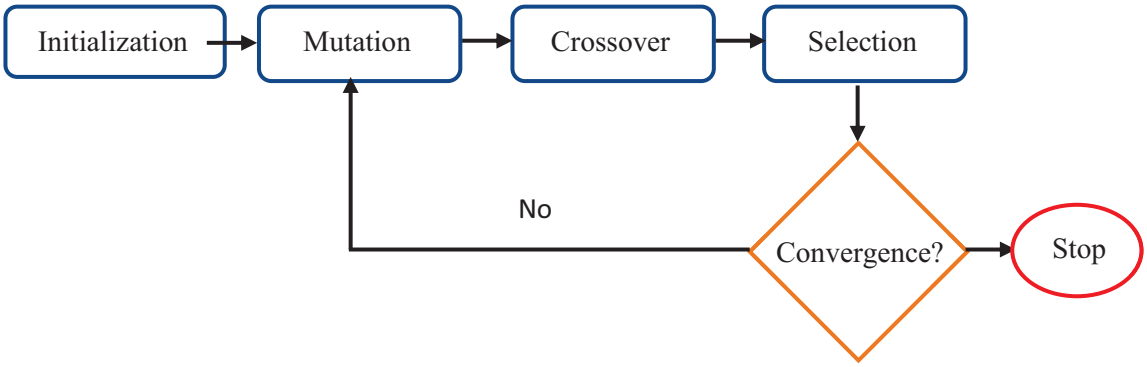

Figure 4.3. The flowchart of Differential Evolution optimization algorithm

4.4.4. Simulated Annealing (SA)

An efficient and general type of optimization is Simulated Annealing (SA). In the presence of large quantities of local optima, it is useful in finding global optima. 'Annealing' refers to a thermodynamic analogy, precisely to the manner in which metals cool and anneal. Simulated annealing instead of the energy of a material uses the objective function of an optimization problem. SA implementation is surprisingly fast. The algorithm is essentially hill-climbing, except that it chooses a random move instead of choosing the right move. The flowchart of the Simulated Annealing algorithm is shown in Figure 4.4.

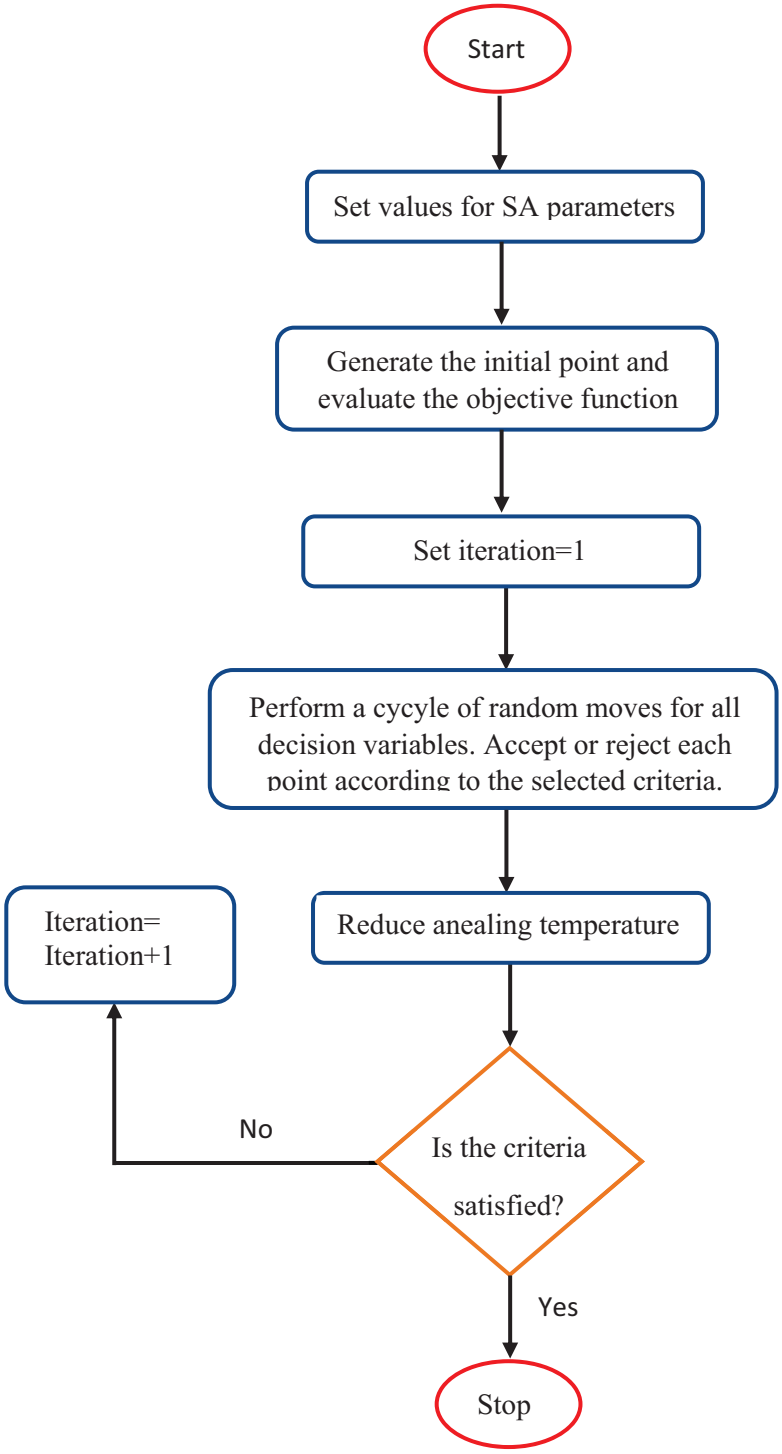

Figure 4.4. The flowchart of Simulated Annealing optimization algorithm

CHAPTER 5

RESULTS AND DISCUSSION

5.1. Problem Statement

Determining the buckling load capacity of a composite plate under in-plane compressive loads is critical to the design of composite structures because buckling can cause failure of the structure. Accordingly, the aim of the thesis is to design the best laminated composite plates that can resist buckling at different loadings and plate dimensions. The composite plates in question are rectangular in shape, simply supported by four sides of length and width, and are subjected to in-plane loads per unit length, as shown in Figure 5.1.

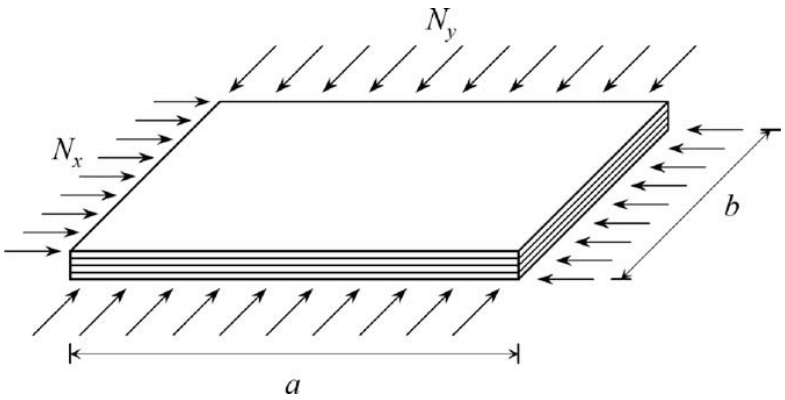

Figure 5.1. Laminated composite subjected to in-plane loads

(Source: Lopez, et al. 2009)

48 and 64-layered composite plates made of different materials which are graphite/epoxy, flax/epoxy, glass/epoxy, carbon/epoxy, flax/polypropylene, and glass/polyester have been considered in the thesis. Each layer is 0.127 mm thick and the length of plate a equals to 0.508 m. N_x has been taken as 1000 N/mm, 5000 N/mm in the design process. N_y and b have been calculated from the load ratio (N_x / N_y) and the plate aspect ratio (a / b), respectively. The mechanical properties of the materials used in this thesis have been taken from articles in literatüre and given in Table 5.1.

Table 5.1. Mechanical properties of materials

Materials	E_1 (GPa)	E_2 (GPa)	G_{12} (GPa)	ν_{12}
Graphite/Epoxy (Karakaya and Soykasap 2009)	127.6	13.0	6.4	0.30
Glass/Epoxy (António and Hoffbauer 2016)	38.6	8.27	4.14	0.26
Carbon/Epoxy (Duran et al. 2015)	147.0	10.3	7.0	0.27
Flax/Epoxy (Savran and Aydin 2018)	22.8	4.52	1.96	0.43
Flax/PP (Modniks and Andersons 2010)	10.3	2.1	0.68	0.38
Glass/Polyester (Duran et al. 2015)	29.6	10.0	4.1	0.29

The design of composite plate has been studied with different aspect ratios; $a/b=1$, $a/b=2$ and $a/b=1/2$ and different loading ratios; $N_x/N_y=1$, $N_x/N_y=2$, $N_x/N_y=1/2$. Fiber orientation angles of the plate have been taken as design variables and considered continuous ($-90\le\theta\le90$) during the optimization process. The composite plates considered in the thesis are symmetric and balanced. Thus, the number of design variables decreases from 48 to 12 and 64 to 16 for 48 and 64-layered composites, respectively. The rate of increase between these angles is also considered as 45 degrees.

The representation of stacking sequence of 48 and 64-layered composite plates can be given as, respectively:

$$[\pm\theta_1/\pm\theta_2/\pm\theta_3/\pm\theta_4/\pm\theta_5/\pm\theta_6/\pm\theta_7/\pm\theta_8/\pm\theta_9/\pm\theta_{10}/\pm\theta_{11}/\pm\theta_{12}]_s$$

And

$$[\pm\theta_1/\pm\theta_2/\pm\theta_3/\pm\theta_4/\pm\theta_5/\pm\theta_6/\pm\theta_7/\pm\theta_8/\pm\theta_9/\pm\theta_{10}/\pm\theta_{11}/\pm\theta_{12}/\pm\theta_{13}/\pm\theta_{14}/\pm\theta_{15}/\pm\theta_{16}]_s$$

The mathematical representation of the optimization problem for this thesis study can be stated as:

Find: $\{\theta_k\}, \theta_k \in \{-90, 90\},\ k = 1,..., n$

Maximize: Critical buckling load factor (λ_{cb})

Subject to: Compressive in-plane loading

Before optimum designs of composite plates were achieved, validation of the algorithms was carried out using the buckling load factor, specific results from previous studies in the literature. The critical buckling load factor has been used as an objective function in optimization. The objective function for each design has been obtained using the MATHEMATICA software program. Here, the smallest value within λ_b (1, 1), λ_b (1, 2), λ_b (2, 1), and λ_b (2, 2) has been taken as the critical buckling load factor (λ_{cb}).

In addition, different optimization algorithms were used while considering different aspect ratios and different load ratios while making the best design study for 48 and 64 layered composite plates. N_x = 1000 N/m was taken as a constant load and N_y = 500 N/m, 1000 N/m, and 2000 N/m were used according to the ratios. Subsequently, the same process was made at the same rate for N_x = 5000 N/m and N_y was examined as 2500 N/m, 5000 N/m, and 10000 N/m. While the N_x and N_y loads changed, the aspect ratios were changed to 1/2, 1, and 2 respectively. There are nine different design cases under a single load for a single material. Since there are six materials and two different loads in total, 108 codes were run for one optimization method. While conducting these investigations, the buckling conditions were taken into consideration and the behavior of the materials against it was examined over the critical buckling load factor.

5.2. Optimization Results and Evaluation

In thesis study, the laminated composite plates subjected to in-plane loads have been analyzed using the Differential Evolution (DE), Simulated Anneling (SA), and Nelder Mead (NM) optimization methods in MATHEMATICA for the given load ratios and plate aspect ratios. The optimum stacking sequence designs have been investigated considering buckling.

Table 5.2. shows how nine different design cases are organized. Each load and each aspect ratio represent a design case.

Table 5.2. Aspect ratio and load ratio of the design cases

Design Case	Aspect Ratio (a/b)	Load Ratio (N_x/N_y)
DC1a	2	1
DC1b	1	1
DC1c	1/2	1
DC2a	2	2
DC2b	1	2
DC2c	1/2	2
DC3a	2	1/2
DC3b	1	1/2
DC3c	1/2	1/2

It contains the specifications of the article from the literature verified in Table 5.3. This article is Karakaya and Soykasap (2009) that contains 64-layered composite study of Graphite/Epoxy.

Table 5.3. Specification of verification problem

Geometrical	a=508mm, t_{ply}=0.127mm	NL=64 Layers
Material Used	Graphite/Epoxy	
Loading	N_x= 1000 N/m	

First, to indicate that the optimization algorithms are reliable, the algorithms for the objective function (critical buckling load factor) have been validated using some appropriate results from previous studies in the literature. The verification results of the buckling load factor algorithm for the load cases (DC1a-DC3c) stated in Karakaya and Soykasap's (2009) study are given in Table 5.4.

Table 5.4. Verification of the code used in the thesis

Design Case	λ_{CB} (Karakaya and Soykasap)	λ_{CB} (Present Study)
DC1a	695.781	695.949
DC1b	242.823	242.884
DC1c	173,945	173.987
DC2a	1,057.948	1058.192
DC2b	323.764	323.845
DC2c	206.492	206.544
DC3a	412.985	413.088
DC3b	161.882	161.922
DC3c	132.243	132.274

It can be seen from Table 5.4. that the critical buckling load factor values are close to the values given by Karakaya and Soykasap (2009). This means that the present buckling load factor algorithm could yield reliable results.

Table 5.5. shows the optimal designs of 64-layered composite plates of Graphite/Epoxy subjected to 1000 N/m in-plane compressive load. Each optimal stacking order is displayed differently as the aspect ratio and load ratio vary for each design situation. At the same time, two different algorithm solutions which are Differential Evolution and Simulated Annealing were used, and they are specified in the table as DE and SA. In these stacking sequence comparisons, optimum designs of materials with different algorithms have been examined. The same investigations were done for Glass/Epoxy in Table 5.6., Flax/Epoxy in Table 5.7., Flax/PP in Table 5.8., Carbon/Epoxy in Table 5.9., and Glass/Polyester in Table 5.10., respectively.

Table 5.5. Optimum stacking sequence designs based on DE and SA for 64-layered Graphite/Epoxy composite (N_x =1000 N/m)

Material	Design Case	Stacking Sequence (DE)	Stacking Sequence (SA)
Graphite/Epoxy	DC1a	$[90_4 / (90_2 / \pm45)_3 / 90_8 / \pm45 / 90_6]_s$	$[90_2 / \pm45 / 90_{10} / \pm45_2 / 90_6 / \pm45 / 90_6]_s$
	DC1b	$[\pm45_{16}]_s$	$[\pm45_{16}]_s$
	DC1c	$[0_2 / \pm45 / 0_{10} / \pm45 / (\pm45 / 0_6)_2]_s$	$[0_6 / \pm45 / 0_4 / \pm45_2 / 0_4 / \pm45 / 0_6 / \pm45 / 0_2]_s$
	DC2a	$[90_4 / \pm45_5 / 90_8 / \pm45_3 / 90_4]_s$	$[\pm45_2 / 90_4 / (90_2 / \pm45)_4 / (\pm45 / 90_2)_2]_s$
	DC2b	$[\pm45_{16}]_s$	$[\pm45_{16}]_s$
	DC2c	$[0_{16} / \pm45 / 0_6 / (\pm45 / 0_2)_2]_s$	$[0_{16} / \pm45 / 0_6 / \pm45 / 0_2 / \pm45_2]_s$
	DC3a	$[90_{10} / (90_6 / \pm45)_2 / 90_2 / \pm45 / 90_2]_s$	$[90_{16} / \pm45 / 90_6 / (\pm45 / 90_2)_2]_s$
	DC3b	$[\pm45_{16}]_s$	$[\pm45_{16}]_s$
	DC3c	$[(\pm45 / 0_2)_2 / \pm45_2 / 0_8 / (\pm45 / 0_2)_2 / \pm45_2]_s$	$[\pm45 / 0_4 / \pm45 / (\pm45 / 0_2)_3 / 0_2 / \pm45 / (\pm45 / 0_2)_2]_s$

Table 5.6. Optimum stacking sequence designs based on DE and SA for 64-layered Glass/Epoxy composite (N_x =1000 N/m)

Material	Design Case	Stacking Sequence (DE)	Stacking Sequence (SA)
Glass/Epoxy	DC1a	$[90_{14} / \pm45 / 90_4 / \pm45 / 90_8 / \pm45]_s$	$[90_{12} / \pm45 / 90_{10} / \pm45 / 90_4 / \pm45]_s$
	DC1b	$[\pm45_{16}]_s$	$[\pm45_{16}]_s$
	DC1c	$[0_{14} / \pm45 / 0_4 / \pm45 / 0_8 / \pm45]_s$	$[0_{16} / \pm45_2 / 0_6 / \pm45 / 0_2 / \pm45]_s$
	DC2a	$[\pm45 / 90_8 / \pm45 / 90_2 / \pm45_6 / 90_2 / \pm45_2]_s$	$[90_4 / \pm45_2 / 90_4 / \pm45 / 90_2 / \pm45_4 / 90_2 / \pm45_3]_s$
	DC2b	$[\pm45_{16}]_s$	$[\pm45_{15} / 90_2]_s$
	DC2c	$[0_{32}]_s$	$[0_{24} / \pm45 / 0_2 / \pm45_2]_s$
	DC3a	$[90_{32}]_s$	$[90_{28} / \pm45 / 90_2]_s$
	DC3b	$[\pm45_{16}]_s$	$[\pm45_{16}]_s$
	DC3c	$[\pm45 / 0_8 / \pm45 / 0_2 / \pm45_6 / 0_2 / \pm45_2]_s$	$[0_4 / \pm45_2 / 0_2 / \pm45 / 0_4 / \pm45_3 / 0_4 / \pm45_3]_s$

Table 5.7. Optimum stacking sequence designs based on DE and SA for 64-layered Flax/Epoxy composite (N_x =1000 N/m)

Material	Design Case	Stacking Sequence (DE)	Stacking Sequence (SA)
Flax/Epoxy	DC1a	$[90_{16}/\pm45_2/90_2/\pm45_4/90_2]_s$	$[90_{10}/\pm45/90_{10}/\pm45/90_2/\pm45_3]_s$
	DC1b	$[\pm45_{16}]_s$	$[\pm45_{16}]_s$
	DC1c	$[0_{16}/\pm45_2/0_2/\pm45_4/0_2]_s$	$[0_{12}/(0_2/\pm45)_3/(0_2/90_2)_2]_s$
	DC2a	$[(90_2/\pm45)_3/\pm45/90_2/(90_4/\pm45)_2/\pm45_2]_s$	$[90_4/\pm45_3/90_2/\pm45/90_6/(\pm45/90_2)_2/\pm45_2]_s$
	DC2b	$[\pm45_{16}]_s$	$[\pm45_{16}]_s$
	DC2c	$[0_{32}]_s$	$[0_{26}/\pm45_2/90_2]_s$
	DC3a	$[90_{32}]_s$	$[90_{24}/\pm45/90_4/\pm45]_s$
	DC3b	$[\pm45_{16}]_s$	$[\pm45_{16}]_s$
	DC3c	$[(0_4/\pm45_2)_2/\pm45_2/0_4/(0_2/\pm45)_2]_s$	$[0_6/\pm45_4/0_2/\pm45_2/0_4/\pm45_2/0_4]_s$

Table 5.8. Optimum stacking sequence designs based on DE and SA for 64-layered Flax/PP composite (N_x =1000 N/m)

Material	Design Case	Stacking Sequence (DE)	Stacking Sequence (SA)
Flax/PP	DC1a	$[90_{10}/\pm45/90_6/\pm45/90_2/\pm45_2/90_6]_s$	$[90_{12}/\pm45_2/90_6/\pm45/90_4/\pm45_2]_s$
	DC1b	$[\pm45_{16}]_s$	$[\pm45_{16}]_s$
	DC1c	$[0_{10}/(\pm45/0_2)_2/0_{10}/\pm45_2]_s$	$[0_{12}/\pm45/0_4/\pm45_2/0_2/\pm45_3/0_2]_s$
	DC2a	$[(90_2/\pm45)_2/\pm45/90_2/(90_2/\pm45)_2/90_8/\pm45/90_2]_s$	$[(90_2/\pm45)_2/90_4/\pm45_3/90_2/\pm45/90_{10}]_s$
	DC2b	$[\pm45_{16}]_s$	$[\pm45_{13}/0_2/\pm45_2]_s$
	DC2c	$[0_{32}]_s$	$[0_{10}/\pm45/0_{14}/\pm45/90_2/\pm45]_s$
	DC3a	$[90_{32}]_s$	$[90_{18}/(\pm45/90_4)_2/0_2]_s$
	DC3b	$[\pm45_{16}]_s$	$[\pm45_{14}/90_2/\pm45]_s$
	DC3c	$[\pm45/(\pm45/0_4)_2/(0_6/\pm45)_2/\pm45]_s$	$[0_4/\pm45/0_2/\pm45_2/0_2/\pm45_3/0_4/\pm45_3/0_2]_s$

Table 5.9. Optimum stacking sequence designs based on DE and SA for 64-layered Carbon/Epoxy composite (N_x =1000 N/m)

Material	Design Case	Stacking Sequence (DE)	Stacking Sequence (SA)
Carbon/Epoxy	DC1a	$[90_{10} / \pm45_4 / 90_2 / \pm45_3 / 90_2 / \pm45]_s$	$[90_4 / \pm45 / 90_6 / \pm45 / 90_2 / \pm45_2 / 90_4 / \pm45_4]_s$
	DC1b	$[\pm45_{16}]_s$	$[\pm45_{16}]_s$
	DC1c	$[0_2 / \pm45 / 0_6 / \pm45 / 0_8 / \pm45_6]_s$	$[0_8 / \pm45 / 0_2 / \pm45_3 / 0_4 / \pm45_4 / 0_2]_s$
	DC2a	$[\pm45_2 / 90_2 / \pm45 / 90_6 / \pm45_2 / 90_{12} / \pm45]_s$	$[\pm45/90_2/\pm45_2/90_6/\pm45/90_2 / \pm45_2 /90_2/\pm45 /90_6]_s$
	DC2b	$[\pm45_{16}]_s$	$[\pm45_{16}]_s$
	DC2c	$[0_{14} / \pm45 / 0_4 / \pm45_2 / 0_6 / \pm45]_s$	$[0_{12} / \pm45 / 0_8 / \pm45_2 / 0_4 / \pm45]_s$
	DC3a	$[90_{14} / \pm45 / 90_2 /\pm45 / 90_6 /\pm45_2 / 90_2]_s$	$[90_{12} / \pm45 / 90_6 /\pm45 / 90_6 /\pm45_2]_s$
	DC3b	$[\pm45_{16}]_s$	$[\pm45_{16}]_s$
	DC3c	$[\pm45_2 / 0_4 / \pm45 / (0_2 /\pm45 /0_2)_2 / \pm45 / 0_8]_s$	$[\pm45_2 / 0_2 / \pm45 / 0_4 / (0_2 /\pm45)_2 / 0_2 / (0_2 /\pm45)_2 / 0_2]_s$

Table 5.10. Optimum stacking sequence designs based on DE and SA for 64-layered Glass/Polyester composite (N_x =1000 N/m)

Material	Design Case	Stacking Sequence (DE)	Stacking Sequence (SA)
Glass/Polyester	DC1a	$[90_{32}]_s$	$[90_{26} / \pm45 / 90_2 / \pm45]_s$
	DC1b	$[\pm45_{16}]_s$	$[\pm45_{14} / 90_2 / \pm45]_s$
	DC1c	$[0_{32}]_s$	$[0_{22} / \pm45_2/90_2/\pm45/90_2]_s$
	DC2a	$[90_4 / \pm45 / 90_6 / \pm45_3 / 90_4 / \pm45 / 90_8]_s$	$[(90_2/\pm45/90_2)_2/90_6/\pm45_2/90_4 /\pm45/90_4]_s$
	DC2b	$[\pm45_{16}]_s$	$[\pm45_{16}]_s$
	DC2c	$[0_{32}]_s$	$[0_{20} / \pm45 / 0_8 / \pm45]_s$
	DC3a	$[90_{32}]_s$	$[90_{24} / \pm45 / 90_2 / 0_2 / \pm45]_s$
	DC3b	$[\pm45_{16}]_s$	$[\pm45_{16}]_s$
	DC3c	$[0_4 / \pm45_2 / 0_6 / (0_2 /\pm45 /0_2)_2 / \pm45 / 0_4]_s$	$[0_6 / \pm45_2 / 0_4 / \pm45 / 0_4 / (\pm45_2 /0_2)_2]_s$

As it is seen from the Table 5.5. – Table 5.10. that DE and SA the optimization algorithm in the stacking sequences cause changes in their designs. It is also seen that geometry (aspect ratio) is a very important factor in design cases.

On the contrary the study done in the previous five tables, stacking sequence designs of six different materials under 5000N compressive load were examined. Table 5.11 shows the optimal designs of 64-layer composite plates of Graphite/Epoxy material under 5000 N/m in-plane compressive load. Unlike 1000N/m, this time it was solved with only one method which is Differential Evolution. The reason is that when comparing 64-layered composites, a critical buckling load factor comparison will be made using the DE algorithm under 1000 N/m and 5000 N/m compressive load. The same process was done and results are given for Glass/Epoxy in Table 5.12, Flax/Epoxy in Table 5.13, Flax/PP in Table 5.14, Carbon/Epoxy in Table 5.15, and Glass/Polyester in Table 5.16, respectively.

Table 5.11. Optimum stacking sequence designs based on DE for 64-layered Graphite/Epoxy composite (N_x =5000 N/m)

Material	Design Case	Stacking Sequence (DE)
Graphite/Epoxy	DC1a	$[90_4 / (90_2 / \pm45)_3 / 90_8 / \pm45 / 90_6]_s$
	DC1b	$[\pm45_{16}]_s$
	DC1c	$[0_2 / \pm45 / 0_{10} / \pm45 / (\pm45 / 0_6)_2]_s$
	DC2a	$[90_4 / \pm45_5 / 90_8 / \pm45_3 / 90_4]_s$
	DC2b	$[\pm45_{16}]_s$
	DC2c	$[0_{16} / \pm45 / 0_6 / (\pm45 / 0_2)_2]_s$
	DC3a	$[90_{10} / (90_6 / \pm45)_2 / 90_2 / \pm45 / 90_2]_s$
	DC3b	$[\pm45_{16}]_s$
	DC3c	$[(\pm45 / 0_2)_2 / \pm45_2 / 0_8 / (\pm45 / 0_2)_2 / \pm45_2]_s$

Table 5.12. Optimum stacking sequence designs based on DE for 64-layered Glass/Epoxy composite (N_x =5000 N/m)

Material	Design Case	Stacking Sequence (DE)
Glass/Epoxy	DC1a	$[90_{14} / \pm45 / 90_4 / \pm45 / 90_8 / \pm45]_s$
	DC1b	$[\pm45_{16}]_s$
	DC1c	$[0_2 / \pm45 / 0_{10} / \pm45 / (\pm45 / 0_6)_2]_s$
	DC2a	$[\pm45 / 90_8 / \pm45 / 90_2 / \pm45_6 / 90_2 / \pm45_2]_s$
	DC2b	$[\pm45_{16}]_s$
	DC2c	$[0_{32}]_s$
	DC3a	$[90_{10} / (90_6 / \pm45)_2 / 90_2/\pm45 / 90_2]_s$
	DC3b	$[\pm45_{16}]_s$
	DC3c	$[\pm45 / 0_8 / \pm45 / 0_2 / \pm45_6 / 0_2 / \pm45_2]_s$

Table 5.13. Optimum stacking sequence designs based on DE for 64-layered Flax/Epoxy composite (N_x =5000 N/m)

Material	Design Case	Stacking Sequence (DE)
Flax/Epoxy	DC1a	$[90_{16} /\pm45_2/ 90_2/ \pm45_4/90_2]_s$
	DC1b	$[\pm45_{16}]_s$
	DC1c	$[0_{16}/\pm45_2/0_2/\pm45_4 /0_2]_s$
	DC2a	$[(90_2 /\pm45)_3/ \pm45 / 90_2/ (90_4/\pm45)_2/\pm45_2]_s$
	DC2b	$[\pm45_{16}]_s$
	DC2c	$[0_{32}]_s$
	DC3a	$[90_{32}]_s$
	DC3b	$[\pm45_{16}]_s$
	DC3c	$[(0_4/\pm45_2)_2/\pm45_2 /0_4/ (0_2/\pm45)_2]_s$

Table 5.14. Optimum stacking sequence designs based on DE for 64-layered Flax/PP composite (N_x =5000 N/m)

Material	Design Case	Stacking Sequence (DE)
Flax/PP	DC1a	$[90_{10}$ / ±45/90_6 / ±45/90_2/±45_2/ $90_6]$
	DC1b	$[\pm45_{16}]_s$
	DC1c	$[0_{10}$ / (±45/ 0_2)$_2$/ 0_{10}/±$45_2]_s$
	DC2a	$[(90_2$ /±45)$_3$/ ±45 / 90_2/ (90_4/±45)$_2$/±$45_2]_s$
	DC2b	$[\pm45_{16}]_s$
	DC2c	$[0_{32}]_s$
	DC3a	$[90_{32}]_s$
	DC3b	$[\pm45_{16}]_s$
	DC3c	$[(0_4$/±45_2)$_2$/±45_2 /0_4/ (0_2/±45)$_2]_s$

Table 5.15. Optimum stacking sequence designs based on DE for 64-layered Carbon/Epoxy composite (N_x =5000 N/m)

Material	Design Case	Stacking Sequence (DE)
Carbon/Epoxy	DC1a	$[90_{10}$ / ±45_4 / 90_2 / ±45_3 / 90_4 / ±45$]_s$
	DC1b	$[\pm45_{16}]_s$
	DC1c	$[90_{10}$ / ±45_4 / 90_2 / ±45_3 / 90_4 / ±45$]_s$
	DC2a	$[\pm45_2$ / 90_2 / ±45 / 90_6 / ±45_2 / 90_{12} / ±45$]_s$
	DC2b	$[\pm45_{16}]_s$
	DC2c	$[0_{14}$ / ±45 / 0_4 / ±45_2 / 0_6 / ±45$]_s$
	DC3a	$[90_{14}$ / ±45 / 90_2 / ±45 / 90_6 / ±45_2 / $90_2]_s$
	DC3b	$[\pm45_{16}]_s$
	DC3c	$[\pm45_2$ / 0_4 / ±45 / (0_2 /±45 /0_2)$_2$ / ±45 / $0_8]_s$

Table 5.16. Optimum stacking sequence designs based on DE for 64-layered Glass/Polyester composite (N_x =5000 N/m)

Material	Design Case	Stacking Sequence (DE)
Glass/Polyester	DC1a	$[90_{32}]_s$
	DC1b	$[\pm 45_{16}]_s$
	DC1c	$[0_{32}]_s$
	DC2a	$[90_4 / \pm 45 / 90_6 / \pm 45_3 / 90_4 / \pm 45 / 90_8]_s$
	DC2b	$[\pm 45_{16}]_s$
	DC2c	$[0_{32}]_s$
	DC3a	$[90_{32}]_s$
	DC3b	$[\pm 45_{16}]_s$
	DC3c	$[0_4 / \pm 45_2 / 0_6 / (0_2 / \pm 45 / 0_2)_2 / \pm 45 / 0_4]_s$

By comparing the effects of Differential Evolution algorithm in design between Tables 5.5. - 5.10. and Tables 5.11. - 5.16., it can be seen that geometry of the plates is the more effective factor on the design than loads. When the designs of each material were examined, it was seen that even if they were under different loads, they would have the same stacking sequences. It is also obvious that in structures where a and b values are equal, the sequences are the same under each load.

Stacking sequence designs of 64-layered composites were investigated in previous parts. In the next six tables, the stacking sequence designs of 48-layered composite plates will be examined. Table 5.17. indicates the optimal designs of 48-layered composite plates of Graphite/Epoxy under 1000 N/m in-plane compressive load. At the same time, two different algorithm solutions which are Differential Evolution and Simulated Annealing were made, and they are specified in the table as DE and SA. The reason for this is to find the answer to the question of whether it can obtain different stacking sequence designs by using different optimization algorithms.

The same analyzing was done for Glass/Epoxy in Table 5.18., Flax/Epoxy in Table 5.19., Flax/PP in Table 5.20., Carbon/Epoxy in Table 5.21., and Glass/Polyester in Table 5.22., respectively.

Table 5.17. Optimum stacking sequence designs based on DE and SA for 48-layered Graphite/Epoxy composite (N_x =1000 N/m)

Material	Design Case	Stacking Sequence (DE)	Stacking Sequence (SA)
Graphite/Epoxy	DC1a	$[90_4 / \pm45/ 90_6 / \pm45_2/ (90_2/\pm45)_2]_s$	$[90_8 / \pm45_3 / 90_2 / \pm45_2 /90_2 / \pm45]_s$
	DC1b	$[\pm45_{12}]_s$	$[\pm45_{12}]_s$
	DC1c	$[0_8 / \pm45/ (\pm45_2/0_2)_2/\pm45]_s$	$[0_8 / \pm45_3 / 0_2 / \pm45_2 / 0_2 / \pm45]_s$
	DC2a	$[(\pm45 / 90_2)_2/ (90_2 /\pm45)_2/ (\pm45 / 90_2)_2]_s$	$[\pm45/ 90_4/ \pm45_2/ 90_2/ \pm45 /90_4 /\pm45_2 /90_2]_s$
	DC2b	$[\pm45_{12}]_s$	$[\pm45_{12}]_s$
	DC2c	$[0_{12} /\pm45 / 0_{10}]_s$	$[0_{12} / \pm45 / 0_{10}]_s$
	DC3a	$[90_{12} / \pm45/ 90_{10}]_s$	$[90_{12} / \pm45 / 90_{10}]_s$
	DC3b	$[\pm45_{12}]_s$	$[\pm45_{12}]_s$
	DC3c	$[0_2 / \pm45/ (\pm45/0_2)_4/0_2 / \pm45]_s$	$[(0_2 / \pm45)_s / (\pm45 / 0_2)_3 / 0_2 / \pm45]_s$

Table 5.18. Optimum stacking sequence designs based on DE and SA for 48-layered Glass/Epoxy composite (N_x =1000 N/m)

Material	Design Case	Stacking Sequence (DE)	Stacking Sequence (SA)
Glass/Epoxy	DC1a	$[90_{12}/(\pm45/90_2)_2/90_2/\pm45]_s$	$[90_{12}/(\pm45/90_2)_2/90_2/\pm45]_s$
	DC1b	$[\pm45_{12}]_s$	$[\pm45_{12}]_s$
	DC1c	$[0_{12}/(\pm45/0_2)_2/0_2/\pm45]_s$	$[0_{12}/\pm45/0_2/\pm45/0_2/\pm45_2]_s$
	DC2a	$[(90_2/\pm45)_4/90_4/\pm45/90_2]_s$	$[(90_2/\pm45)_4/90_4/\pm45/90_2]_s$
	DC2b	$[\pm45_{12}]_s$	$[\pm45_{12}]_s$
	DC2c	$[0_{24}]_s$	$[0_{20}/\pm45_2]_s$
	DC3a	$[90_{24}]_s$	$[90_{22}/\pm45]_s$
	DC3b	$[\pm45_{12}]_s$	$[\pm45_{12}]_s$
	DC3c	$[(0_2/\pm45)_4/0_4/\pm45/0_2]_s$	$[(\pm45/0_4)_2/\pm45/0_2/\pm45/0_4/\pm45]_s$

Table 5.19. Optimum stacking sequence designs based on DE and SA for 48-layered Flax/Epoxy composite (N_x =1000 N/m)

Material	Design Case	Stacking Sequence (DE)	Stacking Sequence (SA)
Flax/Epoxy	DC1a	$[90_8/\pm45/90_{10}/\pm45_2]_s$	$[90_{12}/(\pm45_2/90_2)_2]_s$
	DC1b	$[\pm45_{12}]_s$	$[\pm45_{12}]_s$
	DC1c	$[0_{12}/(\pm45_2/0_2)_2]_s$	$[0_{18}/90_2/0_2/90_2]_s$
	DC2a	$[90_4/\pm45_2/(\pm45/90_2)_2/(90_2/\pm45)_2]_s$	$[(\pm45/90_4)_2/\pm45/90_2/\pm45_3/90_2]_s$
	DC2b	$[\pm45_{12}]_s$	$[\pm45_{12}]_s$
	DC2c	$[0_{24}]_s$	$[0_{12}/\pm45_2/0_2/\pm45_3]_s$
	DC3a	$[90_{24}]_s$	$[90_{24}]_s$
	DC3b	$[\pm45_{12}]_s$	$[\pm45_{10}/0_2/\pm45]_s$
	DC3c	$[0_4/\pm45_2/0_2/\pm45_3/0_6/\pm45]_s$	$[(\pm45/0_2)_2/0_6/\pm45_2/0_4/\pm45]_s$

Table 5.20. Optimum stacking sequence designs based on DE and SA for 48-layered Flax/PP composite (N_x =1000 N/m)

Material	Design Case	Stacking Sequence (DE)	Stacking Sequence (SA)
Flax/PP	DC1a	$[90_6/ \pm45 /90_{10} /\pm45 /90_4]_s$	$[90_8 / \pm45 / 90_4 / \pm45/ 90_4 / \pm45 / 90_2]_s$
	DC1b	$[\pm45_{12}]_s$	$[\pm45_{12}]_s$
	DC1c	$[0_6 / \pm45/ 0_{10} / \pm45/ 0_4]_s$	$[0_8 / \pm45 / 0_6 / \pm45_2 / 0_2 / \pm45]_s$
	DC2a	$[90_2/ \pm45_2 /90_4 / (90_2 / \pm45_2)_2 /90_2]_s$	$[\pm45 / 90_6 / \pm45_2 / 90_2 / \pm45 / 90_2 /\pm45_2 / 90_2]_s$
	DC2b	$[\pm45_{12}]_s$	$[\pm45_{12}]_s$
	DC2c	$[0_{24}]_s$	$[0_{12} / \pm45 / 0_4 / \pm45_3]_s$
	DC3a	$[90_{24}]_s$	$[90_{18} / \pm45_2 / 90_2]_s$
	DC3b	$[\pm45_{12}]_s$	$[\pm45_{12}]_s$
	DC3c	$[0_2/\pm45_2 / 0_6/ (\pm45_2/0_2)_2]_s$	$[0_4 / \pm45 / 0_2 / \pm45_8]_s$

Table 5.21. Optimum stacking sequence designs based on DE and SA for 48-layered Carbon/Epoxy composite (N_x =1000 N/m)

Material	Design Case	Stacking Sequence (DE)	Stacking Sequence (SA)
Carbon/Epoxy	DC1a	$[(90_4 / \pm45)_2 / 90_2 / \pm45_2 / 90_4 / \pm45]_s$	$[90_4 / \pm45 / 90_2 / \pm45 / 90_6 / \pm45_2 / 90_2 / \pm45]_s$
	DC1b	$[\pm45_{12}]_s$	$[\pm45_{12}]_s$
	DC1c	$[0_6 / \pm45_2 / 0_2 / \pm45 / 0_4 / \pm45 / 0_2 /\pm45]_s$	$[0_4 / \pm45 / 0_2 / \pm45 / 0_6 / \pm45_2 / 0_2 /\pm45]_s$
	DC2a	$[90_4/\pm45_5 /(90_2/\pm45_2)_2]_s$	$[\pm45/90_2/\pm45_2/90_6/\pm45/ 90_2/\pm45_2/90_2]_s$
	DC2b	$[\pm45_{12}]_s$	$[\pm45_{12}]_s$
	DC2c	$[0_{12} / \pm45 / 0_2 / \pm45_4]_s$	$[0_{12} / \pm45 / 0_2 / \pm45_4]_s$
	DC3a	$[90_{12} / \pm45 / 90_2 /\pm45_4]_s$	$[90_{12} / \pm45 / 90_2 / \pm45_4]_s$
	DC3b	$[\pm45_{12}]_s$	$[\pm45_{12}]_s$
	DC3c	$[0_4 /\pm45_5 / 0_2 / \pm45_2 / 0_2 /\pm45]_s$	$[0_4 /\pm45_5 / 0_2 / \pm45_2 / 0_2 /\pm45]_s$

Table 5.22. Optimum stacking sequence designs based on DE and SA for 48-layered Glass/Polyester composite (N_x =1000 N/m)

Material	Design Case	Stacking Sequence (DE)	Stacking Sequence (SA)
Glass/Polyester	DC1a	$[90_{24}]_s$	$[90_{22} / 0_2]_s$
	DC1b	$[\pm 45_{12}]_s$	$[\pm 45_{12}]_s$
	DC1c	$[0_{24}]_s$	$[0_{16} / \pm 45 / 0_2 / \pm 45_2]_s$
	DC2a	$[90_6 / \pm 45_2 / 90_2 / \pm 45 / 90_2 / \pm 45_2 / 90_2 / \pm 45]_s$	$[(90_4 / \pm 45)_2 / (\pm 45 / 90_2)_2 / \pm 45_2]_s$
	DC2b	$[\pm 45_{12}]_s$	$[\pm 45_{12}]_s$
	DC2c	$[0_{24}]_s$	$[0_{24}]_s$
	DC3a	$[90_{24}]_s$	$[90_{22} / 0_2]_s$
	DC3b	$[\pm 45_{12}]_s$	$[\pm 45_{12}]_s$
	DC3c	$[0_4 / \pm 45 / 0_4 / \pm 45_2 / 0_2 / \pm 45 / 0_2 / \pm 45_2]_s$	$[(\pm 45 / 0_8)_2 / \pm 45_2]_s$

When examined between Table 5.17. and Table 5.22., although the same compressive load was applied to the plates, design solutions were made with different optimization algorithms. This use of different algorithms also showed that the designs can change, although it can achieve similar results in some geometries in the design.

In the results so far, 1000 N/m and 5000 N/m examinations were performed for 64 layered composites, the same process was examined with 1000 N/m application for 48 layered composites. In the next studies, a solution will be made to 48 layered composites with 5000 N/m application and two different optimization algorithms. Table 5.23. demonstrates the optimal designs of 48 layered composite plates of Graphite/Epoxy material under 5000 N/m in-plane compressive load. At the same time, different algorithm solutions were made, and they are specified in the table as DE and NM. Previously, comparisons of DE and SA were examined in both 64 layered and 48 layered composite plates under 1000 N/m in-plane compressive load. In this instance, a comparison between DE and NM effect will be made. The same was done for Glass/Epoxy in Table 5.24., Flax/Epoxy in Table 5.25., Flax/PP in Table 5.26., Carbon/Epoxy in Table 5.27., and Glass/Polyester in Table 5.28., respectively.

Table 5.23. Optimum stacking sequence designs based on DE and NM for 48-layered Graphite/Epoxy composite (N_x =5000 N/m)

Material	Design Case	Stacking Sequence (DE)	Stacking Sequence (NM)
Graphite/Epoxy	DC1a	$[90_4 / \pm45/ 90_6 / \pm45_2/ (90_2/\pm45)_2]_s$	$[90_8 / \pm45_3 / 90_2 / \pm45_2/ 90_2/\pm45]_s$
	DC1b	$[\pm45_{12}]_s$	$[\pm45_{12}]_s$
	DC1c	$[0_8 / \pm45/(\pm45_2/0_2)_2/\pm45]_s$	$[0_6 / \pm45_2/ 0_6/\pm45_2/0_2/ \pm45]_s$
	DC2a	$[(\pm45 / 90_2)_2/ (90_2 /\pm45)_2/ (\pm45 / 90_2)_2]_s$	$[90_2/ \pm45_2/ 90_2/ \pm45/90_4/ \pm45_5]_s$
	DC2b	$[\pm45_{12}]_s$	$[\pm45_{12}]_s$
	DC2c	$[0_{12} /\pm45 / 0_{10}]_s$	$[0_{14} /\pm45/0_2/\pm45_3]_s$
	DC3a	$[90_{12} / \pm45/ 90_{10}]_s$	$[90_{12} / \pm45/ 90_{10}]_s$
	DC3b	$[\pm45_{12}]_s$	$[\pm45_{12}]_s$
	DC3c	$[0_2/\pm45/(\pm45/0_2)_4/0_2/\pm45]_s$	$[0_4 /\pm45_5/ 0_4/\pm45_3]_s$

Table 5.24. Optimum stacking sequence designs based on DE and NM for 48-layered Glass/Epoxy composite (N_x =5000 N/m)

Material	Design Case	Stacking Sequence (DE)	Stacking Sequence (NM)
Glass/Epoxy	DC1a	$[90_{12} / (\pm45 / 90_2)_2/90_2 /\pm45]_s$	$[90_{12} / (\pm45 / 90_2)_2/90_4]_s$
	DC1b	$[\pm45_{12}]_s$	$[\pm45_{12}]_s$
	DC1c	$[0_{12} /(\pm45/0_2)_2/0_2/\pm45]_s$	$[0_{14} /\pm45_5]_s$
	DC2a	$[(90_2/\pm45)_4/90_4/\pm45/90_2]_s$	$[(90_2 / \pm45)_4/ 90_4 / \pm45_2]_s$
	DC2b	$[\pm45_{12}]_s$	$[\pm45_{12}]_s$
	DC2c	$[0_{24}]_s$	$[0_{18}/\pm45/0_4]_s$
	DC3a	$[90_{24}]_s$	$[90_{24}]_s$
	DC3b	$[\pm45_{12}]_s$	$[\pm45_{12}]_s$
	DC3c	$[(0_2 / \pm45)_4/ 0_4 / \pm45/0_2]_s$	$[0_4/\pm45/0_2/\pm45_4//0_2/\pm45_3]_s$

Table 5.25. Optimum stacking sequence designs based on DE and NM for 48-layered Flax/Epoxy composite (N_x =5000 N/m)

Material	Design Case	Stacking Sequence (DE)	Stacking Sequence (NM)
Flax/Epoxy	DC1a	$[90_4 / \pm45_3 / 90_2/\pm45 /90_4/\pm45/90_2/\pm45]_s$	$[90_{10} / \pm45/ 90_4/\pm45_2/90_4]_s$
	DC1b	$[\pm45_{12}]_s$	$[\pm45_{12}]_s$
	DC1c	$[0_{12} / (\pm45_2/0_2)_2]_s$	$[0_{12} / (\pm45_2/0_2)_2]_s$
	DC2a	$[90_4 / \pm45_3 / 90_2/\pm45 /90_4/\pm45/90_2/\pm45]_s$	$[\pm45/90_6/\pm45_2/90_4/\pm45_4]_s$
	DC2b	$[\pm45_{12}]_s$	$[\pm45_{12}]_s$
	DC2c	$[0_{24}]_s$	$[0_{18}/\pm45/0_4]_s$
	DC3a	$[90_{24}]_s$	$[90_{24}]_s$
	DC3b	$[\pm45_{12}]_s$	$[\pm45_{12}]_s$
	DC3c	$[(\pm45/0_4)_2/\pm45/0_2/\pm45_3/0_2]_s$	$[0_4/\pm45/0_2/\pm45_5/0_2/\pm45_2]_s$

Table 5.26. Optimum stacking sequence designs based on DE and NM for 48-layered Flax/PP composite (N_x =5000 N/m)

Material	Design Case	Stacking Sequence (DE)	Stacking Sequence (NM)
Flax/PP	DC1a	$[90_6 / \pm45 / 90_{10} / \pm45/90_4]_s$	$[90_6 / \pm45 / 90_{10} / \pm45/90_4]_s$
	DC1b	$[\pm45_{12}]_s$	$[\pm45_{12}]_s$
	DC1c	$[0_6 / \pm45/ 0_{10}/\pm45/0_4]_s$	$[0_8 / \pm45/ 0_6/\pm45_4]_s$
	DC2a	$[90_2/\pm45_2/90_6/(\pm45_2/90_2)_2]_s$	$[90_4 /\pm45_3 / 90_4/\pm45_4/90_2]_s$
	DC2b	$[\pm45_{12}]_s$	$[\pm45_{12}]_s$
	DC2c	$[0_{24}]_s$	$[0_{18}/\pm45/0_4]_s$
	DC3a	$[90_{24}]_s$	$[90_{24}]_s$
	DC3b	$[\pm45_{12}]_s$	$[\pm45_{12}]_s$
	DC3c	$[0_2/\pm45_2 / 0_6/(\pm45_2 /0_2)_2]_s$	$[(\pm45/0_4/\pm45/0_2)_2/0_2/\pm45]_s$

Table 5.27. Optimum stacking sequence designs based on DE and NM for 48-layered Carbon/Epoxy composite (N_x =5000 N/m)

Material	Design Case	Stacking Sequence (DE)	Stacking Sequence (NM)
Carbon/Epoxy	DC1a	$[(90_4 / \pm45)_2 /90_2/\pm45_2 / 90_4 / \pm45]_s$	$[(90_4 / \pm45)_2 /\pm45/ 90_6/\pm45_2]_s$
	DC1b	$[\pm45_{12}]_s$	$[\pm45_{12}]_s$
	DC1c	$[0_6 /\pm45_2 / (0_2 /\pm45 /0_2)_2 / \pm45]_s$	$[0_2 /\pm45/0_8/ \pm45_2 /(0_2 /\pm45)_2]_s$
	DC2a	$[90_4 / \pm45_5 / 90_2 / \pm45_2 / 90_2 /\pm45]_s$	$[\pm45/90_4/\pm45_2/90_2/\pm45/90_2 /\pm45_2/90_2/\pm45]_s$
	DC2b	$[\pm45_{12}]_s$	$[\pm45_{12}]_s$
	DC2c	$[0_{12} / \pm45 / 0_2 / \pm45_4]_s$	$[0_{12} / \pm45 / 0_2 / \pm45_4]_s$
	DC3a	$[90_{12} / \pm45 / 90_2 / \pm45_4]_s$	$[90_{12} / \pm45 / 90_2 / \pm45_4]_s$
	DC3b	$[\pm45_{12}]_s$	$[\pm45_{12}]_s$
	DC3c	$[0_4 / \pm45_5 /0_2 / \pm45_2 / 0_2 / \pm45]_s$	$[0_2 / \pm45/0_2 / \pm45_2 / 0_2 / \pm45_5/ 0_2]_s$

Table 5.28. Optimum stacking sequence designs based on DE and NM for 48-layered Glass/Polyester composite (N_x =5000 N/m)

Material	Design Case	Stacking Sequence (DE)	Stacking Sequence (NM)
Glass/Polyester	DC1a	$[90_{24}]_s$	$[90_{24}]_s$
	DC1b	$[\pm45_{12}]_s$	$[\pm45_{12}]_s$
	DC1c	$[0_{24}]_s$	$[0_{18}/\pm45/0_4]_s$
	DC2a	$[90_6 / \pm45_2 / 90_2 / \pm45 / 90_2 / \pm45_2 /90_2 / \pm45]_s$	$[90_6 / \pm45 / 90_2 / \pm45_3 / 90_2 /\pm45_3]_s$
	DC2b	$[\pm45_{12}]_s$	$[\pm45_{12}]_s$
	DC2c	$[0_{24}]_s$	$[0_{18}/\pm45/0_4]_s$
	DC3a	$[90_{24}]_s$	$[90_{24}]_s$
	DC3b	$[\pm45_{12}]_s$	$[\pm45_{12}]_s$
	DC3c	$[0_4 / \pm45 / 0_4 / \pm45_2 / 0_2 / \pm45 / 0_2 / \pm45_2]_s$	$[0_6 / \pm45_2/ 0_2 / \pm45 / 0_2 / \pm45_2 / 0_4]_s$

A laminate consists of a group of single layers bonded together. With a reference axis, each layer can be defined by its position in the laminate, its material, and its orientation angle. Each layer is defined by ply angle and separated from the other layers by a slash. The first ply is the top layer of the laminate. Special marks are used for symmetrical laminates, laminates adjacent in the same orientation or at opposite angles, and hybrid laminates. The laminate codes for 48 layers of Carbon / Epoxy and Glass / Polyester are shown in Figures 5.2. and 5.3., respectively to clarify the meaning of stacking sequences presented in Tables.

Laminate Code	Laminate Sequences
$[\pm 45_2]_s$	+45
	-45
	+45
	-45
	+45
	-45
	+45
	-45
	+45
	-45
	+45
	-45
	+45
	-45
	+45
	-45
	+45
	-45
	+45
	-45
	+45
	-45
	+45
	-45
	-45
	+45
	-45
	+45
	-45
	+45
	-45
	+45
	-45
	+45
	-45
	+45
	-45
	+45
	-45
	+45
	-45
	+45
	-45
	+45
	-45
	+45
	-45
	+45
	-45
	+45
	-45
	+45
	-45
	+45
	-45
	+45

Figure 5.2. Representation of Stacking Sequences for 48-Layered Carbon/Epoxy for DC2b

Laminate Code	Laminate Sequences
$[90_6/\pm45_2/90_2/\pm45/90_2/\pm45_2/90_2/\pm45]_s$	90
	90
	90
	90
	90
	90
	+45
	-45
	+45
	-45
	90
	90
	+45
	-45
	90
	90
	+45
	-45
	+45
	-45
	90
	90
	+45
	-45
	-45
	+45
	90
	90
	-45
	+45
	-45
	+45
	90
	90
	-45
	+45
	90
	90
	-45
	+45
	-45
	+45
	90
	90
	90
	90
	90
	90

Figure 5.3. Representation of Stacking Sequences for 48-Layered Glass/Polyester for DC2a

In the last five tables, DE and NM algorithms were compared under the same load. The design similarities can be said more for this comparison than the previous DE and SA comparison. However, it is not correct to compare the designs obtained alone. Likewise, besides the designs, the comparison of the critical buckling load factor should be made, and the most optimal results should be considered.

The most optimum designs for the stacking sequence have been examined in all tables up to last table. While examining these designs, N_x was kept constant for two values as 1000 N/m and 5000 N/m and N_y was decreased or increased at different rates which are 1/2, 1, and 2. While the load ratio was realized, in order to see the geometric effect on the stacking sequences at the same time, the value of "b" was changed by keeping "a" constant and the most optimal designs came out at different rates. In addition to these, the best stacking sequence angles were obtained according to the 3 different optimization algorithms DE, SA, and NM.

After Table 5.29., critical buckling load comparisons of these designs will be made in tables. While conducting these investigations, DE and SA examination for 1000 N/m case of 48 and 64 layered composite plates, DE and NM examination for 5000 N/m case of 48 layered composite plates, and DE examination for 5000 N/m case of 64 layered composite plates. While making comparisons, the values of all critical buckling load factors are given in the tables.

Table 5.29. Critical buckling load factor based on DE and SA for Graphite/Epoxy for 64-layered composites

		N_x = 1000 N		N_x = 5000 N
Material	Design Case	λ_{CB} (DE)	λ_{CB} (SA)	λ_{CB} (DE)
Graphite/Epoxy	DC1a	695.949	695.949	139.189
	DC1b	242.884	242.884	48.576
	DC1c	173.987	173.974	34.797
	DC2a	1058.192	1058.192	211.638
	DC2b	323.845	323.845	64.769
	DC2c	206.544	206.529	41.308
	DC3a	413.088	413.088	82.617
	DC3b	161.922	161.922	32.384
	DC3c	132.274	132.274	26.454

Table 5.30. Critical buckling load factor based on DE and SA for Glass/Epoxy for 64-layered composites

		N_x = 1000 N		N_x = 5000 N
Material	**Design Case**	**λ_{CB} (DE)**	**λ_{CB} (SA)**	**λ_{CB} (DE)**
Glass/Epoxy	DC1a	241.256	241.256	48.251
	DC1b	81.390	81.385	16.278
	DC1c	60.314	60.287	12.062
	DC2a	364.817	364.817	72.963
	DC2b	108.520	108.520	21.704
	DC2c	68.336	68.145	13.667
	DC3a	136.673	136.614	27.334
	DC3b	54.260	54.260	10.852
	DC3c	45.602	45.598	9.120

Table 5.31. Critical buckling load factor based on DE and SA for Flax/Epoxy for 64-layered composites

		N_x = 1000 N		N_x = 5000 N
Material	**Design Case**	**λ_{CB} (DE)**	**λ_{CB} (SA)**	**λ_{CB} (DE)**
Flax/Epoxy	DC1a	143.493	143.484	28.698
	DC1b	48.533	48.533	9.706
	DC1c	35.873	35.790	7.174
	DC2a	217.032	217.032	43.406
	DC2b	64.711	64.711	12.942
	DC2c	40.965	40.891	8.193
	DC3a	81.931	81.731	16.386
	DC3b	32.355	32.355	6.471
	DC3c	27.129	27.129	5.425

Table 5.32. Critical buckling load factor based on DE and SA for Flax/PP for 64-layered composites

		N_x = 1000 N		N_x = 5000 N
Material	Design Case	λ_{CB} (DE)	λ_{CB} (SA)	λ_{CB} (DE)
Flax/PP	DC1a	62.573	62.569	12.514
	DC1b	21.864	21.831	4.372
	DC1c	15.643	15.637	3.128
	DC2a	95.535	95.535	19.107
	DC2b	29.152	29.152	5.830
	DC2c	18.009	18.009	3.601
	DC3a	36.018	35.642	7.203
	DC3b	14.576	14.568	2.915
	DC3c	11.941	11.940	2.388

Table 5.33. Critical buckling load factor based on DE and SA for Carbon/Epoxy for 64-layered composites

		N_x = 1000 N		N_x = 5000 N
Material	**Design Case**	**λ_{CB} (DE)**	**λ_{CB} (SA)**	**λ_{CB} (DE)**
Carbon/Epoxy	DC1a	778.699	778.699	155.739
	DC1b	270.579	270.579	54.115
	DC1c	194.674	194.674	38.934
	DC2a	1181.162	1181.152	236.232
	DC2b	360.772	360.772	72.154
	DC2c	231.542	231.542	46.308
	DC3a	463.085	463.085	92.617
	DC3b	180.386	180.386	36.077
	DC3c	147.645	147.644	29.529

Table 5.34. Critical buckling load factor based on DE and SA for Glass/Polyester for 64-layered composites

		N_x = 1000 N		N_x = 5000 N
Material	**Design Case**	**λ_{CB} (DE)**	**λ_{CB} (SA)**	**λ_{CB} (DE)**
Glass/Polyester	DC1a	200.989	200.791	40.197
	DC1b	69.751	69.725	13.950
	DC1c	50.247	49.860	10.049
	DC2a	313.996	313.996	62.799
	DC2b	93.002	93.002	18.600
	DC2c	55.830	55.576	11.166
	DC3a	111.660	111.353	22.332
	DC3b	46.501	46.501	9.300
	DC3c	39.249	39.241	7.849

Table 5.35. Critical buckling load factor based on DE, SA, and NM for Graphite/Epoxy for 48-layered composites

		N_x = 1000 N		N_x = 5000 N	
Material	Design Case	λ_{CB} (DE)	λ_{CB} (SA)	λ_{CB} (DE)	λ_{CB} (NM)
Graphite/Epoxy	DC1a	293.475	293.566	58.695	58.713
	DC1b	102.466	102.466	20.493	20.493
	DC1c	73.391	73.391	14.678	14.674
	DC2a	446.375	446.375	89.275	89.202
	DC2b	136.622	136.622	27.324	27.325
	DC2c	87.117	87.117	17.423	17.421
	DC3a	174.235	174.235	34.847	34.847
	DC3b	68.311	68.311	13.662	13.662
	DC3c	55.796	55.796	11.159	11.155

Table 5.36. Critical buckling load factor based on DE, SA, and NM for Glass/Epoxy for 48-layered composites

		N_x = 1000 N		N_x = 5000 N	
Material	Design Case	λ_{CB} (DE)	λ_{CB} (SA)	λ_{CB} (DE)	λ_{CB} (NM)
Glass/Epoxy	DC1a	101.757	101.757	20.351	20.347
	DC1b	34.336	34.336	6.867	6.867
	DC1c	25.439	25.423	5.087	5.083
	DC2a	153.897	153.897	30.779	30.778
	DC2b	45.782	45.782	9.156	9.156
	DC2c	28.829	28.795	5.765	5.750
	DC3a	57.659	57.650	11.531	11.531
	DC3b	22.891	22.891	4.578	4.578
	DC3c	19.237	19.237	3.847	3.845

Table 5.37. Critical buckling load factor based on DE, SA, and NM for Flax/Epoxy for 48-layered composites

		N_x = 1000 N		N_x = 5000 N	
Material	Design Case	λ_{CB} (DE)	λ_{CB} (SA)	λ_{CB} (DE)	λ_{CB} (NM)
Flax/Epoxy	DC1a	60.535	60.528	12.107	12.096
	DC1b	20.475	20.475	4.095	4.095
	DC1c	15.132	15.129	3.026	3.026
	DC2a	91.557	91.557	18.311	18.273
	DC2b	27.300	27.300	5.460	5.460
	DC2c	17.282	17.150	3.456	3.446
	DC3a	34.564	34.564	6.912	6.912
	DC3b	13.65	13.633	2.730	2.730
	DC3c	11.444	11.444	2.288	2.287

Table 5.38. Critical buckling load factor based on DE, SA, and NM for Flax/PP for 48-layered composites

		N_x = 1000 N		N_x = 5000 N	
Material	Design Case	λ_{CB} (DE)	λ_{CB} (SA)	λ_{CB} (DE)	λ_{CB} (NM)
Flax/PP	DC1a	26.392	26.388	5.278	5.272
	DC1b	9.224	9.224	1.844	1.844
	DC1c	6.598	6.584	1.319	1.319
	DC2a	40.301	40.301	8.060	8.059
	DC2b	12.298	12.298	2.459	2.459
	DC2c	7.597	7.464	1.519	1.515
	DC3a	15.195	15.136	3.039	3.039
	DC3b	6.149	6.149	1.229	1.229
	DC3c	5.037	5.035	1.007	1.007

Table 5.39. Critical buckling load factor based on DE, SA, and NM for Carbon/Epoxy for 48-layered composites

		N_x = 1000 N		N_x = 5000 N	
Material	Design Case	λ_{CB} (DE)	λ_{CB} (SA)	λ_{CB} (DE)	λ_{CB} (NM)
Carbon/Epoxy	DC1a	328.511	328.511	65.702	65.702
	DC1b	114.150	114.150	22.830	22.830
	DC1c	82.127	82.127	16.425	16.405
	DC2a	498.289	498.289	99.657	99.647
	DC2b	152.200	152.200	30.440	30.440
	DC2c	97.644	97.644	19.528	19.528
	DC3a	195.288	195.288	39.057	39.057
	DC3b	76.100	76.100	15.220	15.220
	DC3c	62.286	62.286	12.457	12.457

Table 5.40. Critical buckling load factor based on DE, SA, and NM for Glass/Polyester for 48-layered composites

		N_x = 1000 N		N_x = 5000 N	
Material	Design Case	λ_{CB} (DE)	λ_{CB} (SA)	λ_{CB} (DE)	λ_{CB} (NM)
Glass/Polyester	DC1a	84.792	84.767	16.958	16.958
	DC1b	29.426	29.426	5.885	5.885
	DC1c	21.198	21.086	4.239	4.230
	DC2a	132.461	132.461	26.492	26.451
	DC2b	39.235	39.235	7.847	7.847
	DC2c	23.553	23.553	4.710	4.700
	DC3a	47.106	47.093	9.421	9.421
	DC3b	19.617	19.617	3.923	3.923
	DC3c	16.557	16.555	3.311	3.311

By between Table 5.29. and Table 5.40, examinations have been made for each material separately for both load and different optimization methods. Now, comparisons of critical buckling load factors of three materials with high stiffness on different methods will be made collectively. Three algorithms which are Differential Evolution, Simulated Annealing, and Nelder Mead will be considered when making these comparisons.

General comparisons of the values between Tables 5.41 and 5.46 are made. While making these comparisons, three materials are considered. The reason for this is to be able to see the differences between the most commonly used materials and to clearly see the differences within the materials with three different optimization methods. 48 and 64 layered composite layers and two different loadings of these three materials are also discussed.

Table 5.41. Comparison of λ_{CB} values for 48 and 64-layered composites for all materials for Design Case 1a (DC1a) N_x=1000 N/m

Material	Optimization Method	λ_{CB} (48-layered)	λ_{CB} (64-layered)
Graphite/Epoxy	DE	293.475	695.949
	SA	293.566	695.949
	NM	-	-
Carbon/Epoxy	DE	328.511	778.699
	SA	328.511	778.699
	NM	-	-
Glass/Epoxy	DE	101.757	241.256
	SA	101.757	241.256
	NM	-	-

Table 5.42. Comparison of λ_{CB} values for 48 and 64-layered composites for all materials for Design Case 2a (DC2a) Nx=1000 N/m

Material	Optimization Method	λ_{CB} (48-layered)	λ_{CB} (64-layered)
Graphite/Epoxy	DE	446.375	1058.192
	SA	446.375	1058.192
	NM	-	-
Carbon/Epoxy	DE	498.289	1181.162
	SA	498.289	1181.152
	NM	-	-
Glass/Epoxy	DE	153.897	364.817
	SA	153.897	364.817
	NM	-	-

Table 5.43. Comparison of λ_{CB} values for 48 and 64-layered composites for all materials for Design Case 3a (DC3a) Nx=1000 N/m

Material	Optimization Method	λ_{CB} (48-layered)	λ_{CB} (64-layered)
Graphite/Epoxy	DE	174.235	413.088
	SA	174.235	413.088
	NM	-	-
Carbon/Epoxy	DE	195.288	463.085
	SA	195.288	463.085
	NM	-	-
Glass/Epoxy	DE	57.659	136.673
	SA	57.650	136.614
	NM	-	-

Table 5.44. Comparison of λ_{CB} values for 48 and 64-layered composites for all materials for Design Case 1a (DC1a) N_x=5000 N/m

Material	Optimization Method	λ_{CB} (48-layered)	λ_{CB} (64-layered)
Graphite/Epoxy	DE	58.695	139.189
	SA	-	-
	NM	58.713	-
Carbon/Epoxy	DE	65.702	155.739
	SA	-	-
	NM	65.702	-
Glass/Epoxy	DE	20.351	48.251
	SA	-	–
	NM	20.347	-

Table 5.45. Comparison of λ_{CB} values for 48 and 64-layered composites for all materials for Design Case 2a (DC2a) Nx=5000 N/m

Material	Optimization Method	λ_{CB} (48-layered)	λ_{CB} (64-layered)
Graphite/Epoxy	DE	89.275	211.638
	SA	-	-
	NM	89.202	-
Carbon/Epoxy	DE	99.657	236.232
	SA	-	-
	NM	99.647	-
Glass/Epoxy	DE	30.779	72.963
	SA	-	–
	NM	30.778	-

Table 5.46. Comparison of λ_{CB} values for 48 and 64-layered composites for all materials for Design Case 3a (DC3a) N_x=5000 N/m

Material	Optimization Method	λ_{CB} (48-layered)	λ_{CB} (64-layered)
Graphite/Epoxy	DE	34.847	82.617
	SA	-	-
	NM	34.847	-
Carbon/Epoxy	DE	39.057	92.617
	SA	-	-
	NM	39.057	-
Glass/Epoxy	DE	11.531	27.334
	SA	-	–
	NM	11.531	-

In the data between Tables 5.41. and 5.46., for 48 layers, when 1000 N force is applied, DE and SA method, when 5000 N load is applied, DE and NM method are taken into consideration. In 64 layers, when 1000 N force is applied, DE and SA methods were used. As a result of the comparisons, it is seen that the results of these three methods coincide with each other when the solution is made under the appropriate input parameters. It can be clearly stated that the critical buckling load factors of 64 layered composite materials are about 2.4 times better. Although the in-plane load increase is reflected in the result linearly, we can say that the layer effect is parabolic. Because let's take Graphite / Epoxy for example, the critical buckling load value in a 64 layered composite structure was 413, while my expectation was 308 in a 48-layer structure, but the result was 174. This shows that this increase is not linear but parabolic.

Table 5.47. is a table created specifically for Nelder Mead (NM), unlike other tables. This table shows that although the Nelder Mead method is a less common method than DE and SA in general, better results can be obtained by using NM with different parameter methods. The parameters changed here consist of the input parameters of NM. In this case, the random seed was set from 0 to 10. In this way, optimization results using

NM were improved. In addition, the overall optimization results, tabulated in the previous sections with NM, are obtained with improved parameters. Since the maximum number of iterations greater than 1000 does not improve the results, it is set to 1000 through the optimization procedure. The changed parameters of NM improved the critical buckling load as seen in Table 5.47.

Table 5.47. Comparison of critical buckling load and optimum stacking sequences with respect to input parameters of NM for DC1a, N_x=5000 N/m, and 48-layered composite.

Material	λ_{CB} (NM-default)	Stacking Sequence (NM-default)	λ_{CB} (NM-changed parameters)	Stacking Sequence (NM-changed parameters)
Carbon/Epoxy	65.607	$[90_8/\pm45_6/90_4]_s$	65.702	$[(90_4/\pm45)_2/\pm45/90_6/\pm45_2]_s$
Glass/Epoxy	20.176	$[90_{12}/\pm45_3/90_6]_s$	20.347	$[90_{12}/(\pm45/90_2)_2/90_4]_s$
Flax/PP	5.208	$[90_{10}/\pm45_4/90_2/\pm45/90_2]_s$	5.272	$[90_6/\pm45/90_{10}/\pm45/90_4]_s$

In order to see the interpretation of the tables graphically, some selected results from Table 5.29. – 5.40. by Differential Evolution Algorithm are presented in Figure 5.4. and Figure 5.5. As can easily be seen in the figures, the highest resistance to buckling was Carbon / Epoxy, while Flax / PP showed the weakest resistance. Moreover, when the figures are examined, it can be understood that the effect of the increase or decrease in force on the buckling load factor is linear.

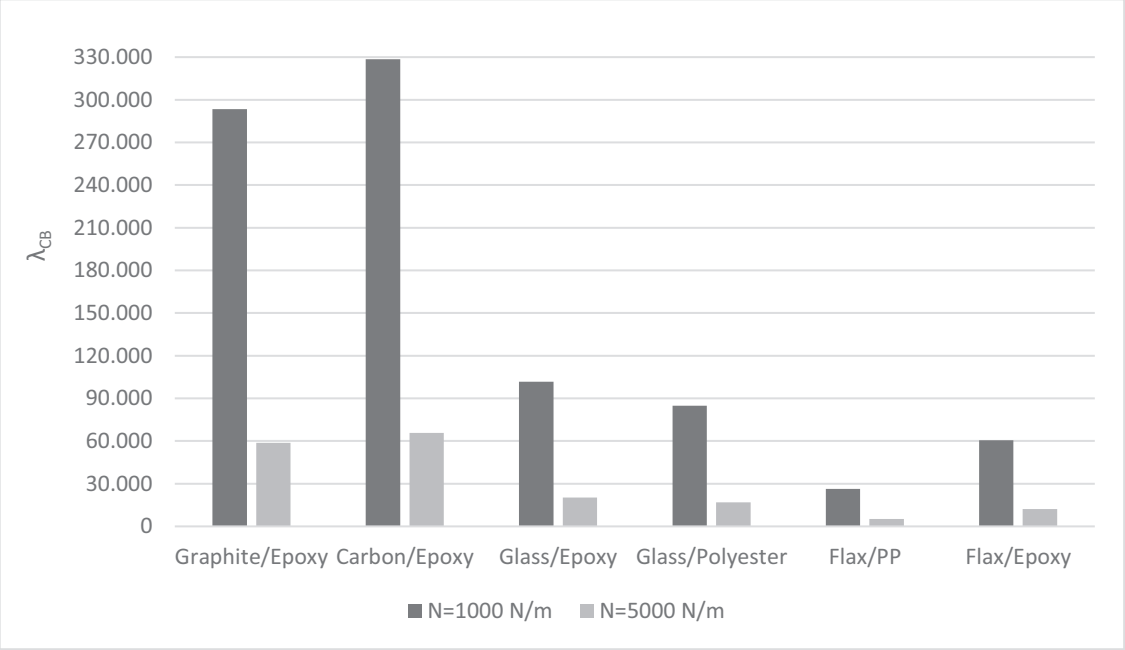

Figure 5.4. Comparison of λ_{CB} values for 48-layered composites for all materials for Design Case 1a (DC1a)

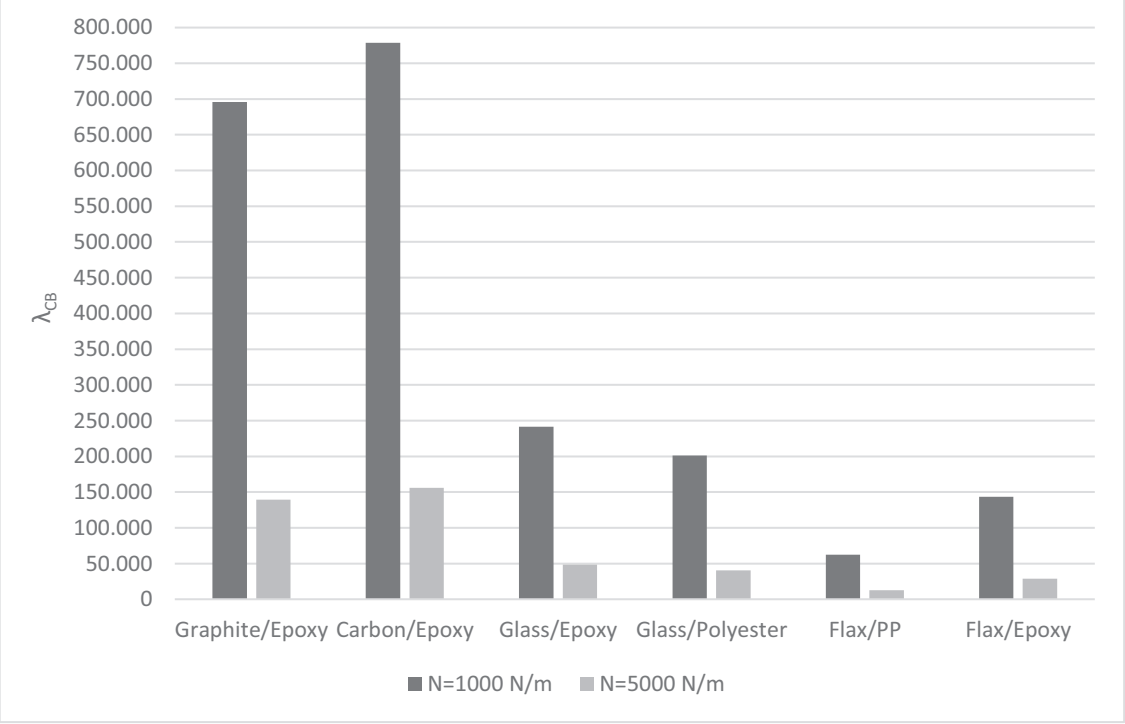

Figure 5.5. Comparison of λ_{CB} values for 64-layered composites for all materials for Design Case 1a (DC1a)

The results of using different methods for 48 and 64 layers of Graphite / Epoxy composite can be seen in Figure 5.6. Despite the use of different methods, the results seem to be very close and consistent. At the same time, when this material with 48 and 64 layers is considered, it is seen that the values increase parabolically. If it had increased linearly; When 293,495 was found in 48 layers, this value would be expected to be 440.5 for 64 layers. However, the result was much higher than expected. Considering these results, it is clear that the layer effect is a crucial factor for buckling studies.

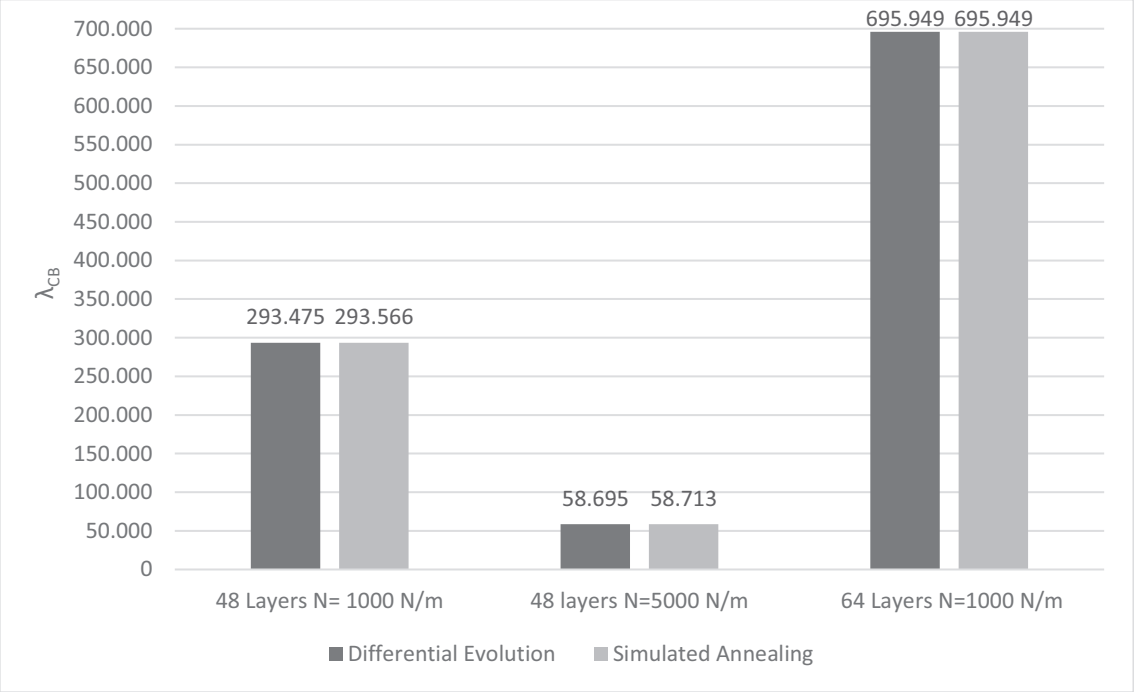

Figure 5.6. Comparison of λ_{CB} values for Graphite/Epoxy for Design Case 1a (DC1a)

CHAPTER 6

CONCLUSION

In this thesis, considering the buckling behavior of six different materials which are graphite/epoxy, carbon/epoxy, glass/epoxy, flax/epoxy, flax/polypropylene, and glass/polyester composite plates with 48 layers and 64 layers, the optimum designs have been examined. Among the optimization methods, three different methods of stochastic optimization methods that are Differential Evolution (DE), Simulated Annealing (SA), and Nelder Mead (NM) were used. MATHEMATICA software program was used in the optimization process. Critical buckling load factor was taken as an objective function and angles of composite plates were taken as design variables. Optimization has been carried out for a variety of different loading conditions and aspect ratios, maximizing the critical buckling load factor for each situation. As the load, N_x was accepted as 1000 N/m and 5000 N/m, while N_y varied according to their rates. Plate length was accepted as 0.508 m, plate width varied according to its proportions. In order to prove the reliability of the code written, the data of the articles taken from the literature have been proved. In order to increase the reliability of the optimization and to obtain the most optimal results, the methods were run in different numbers and at least 1000 iterations were used each time.

Optimum designs in terms of buckling have been obtained as a result of the optimization of the composite plates whose design conditions have been determined. As a beginning, the 64-layered plates of the materials have been optimized for the load of 1000 N/m and 5000 N/m. Subsequently, studies were carried out under the same conditions for 48 layers. The result obtained in both processes revealed that the optimum design of a laminated composite also depends on the loading, loading ratio, and plate aspect ratio. It was observed that the critical buckling load factor values increased with increasing load ratio and plate aspect ratio. From this situation, it can be understood that the in-plane load in the y direction and the plate width “b” are more important parameters in terms of buckling strength.

Optimization of 48-layered composite plates was done to compare with the optimization of 64-layered composite plates. It was observed that the number of reliable composite plate designs and critical buckling load factor values decreased compared to 64 layered designs. As a result, when the material is compared and considering the critical

buckling load factor, it can be easily said that the resisting material to buckling is carbon/epoxy in both 48 and 64-layered composite plates. When we consider glass as fiber material, we can say that epoxy is 16.7% stronger against buckling compared to polyester. If we do the same analysis for flax fiber materials, it is possible to say that epoxy is approximately 56.6% more resistant to buckling than polypropylene.

Finally, when the Simulated Annealing, Differential Evolution, and Nelder Mead methods are compared, it can be clearly said that very similar results were obtained. However, according to the results obtained, the best values were reached by Differential Evolution method. In none of the comparisons, Simulated Annealing and Nelder Mead method did not give better results than Differential Evolution method. However, the results of some cases with Simulated Annealing and Nelder Mead are the same as for Differential Evolution. Other input parameters of NM algorithm being "Shrink Ratio", "Contract Ratio", "Reflect Ratio" and also "Random Seed" were employed with a different value than default. These options decrease the search area of the NM to find better results. It is suggested to try with these changed parameters. Optimization done with NM has been performed with a changed random seed since only changing this parameter affected the results in favor or positively. However, it did not obtain improved results over previous optimum results. In the DE algorithm, changing the input parameter of "Scaling Factor" and "Random Seed" has the potential to positively affect optimization results. However, they could not obtain improved results.

For SA, the input parameter of the "Perturbation Scale" was changed to 3 from 1. However, it found an inferior result compared to its default setting. In general, this parameter increases step size which might improve the result. Another input option, "Boltzmann Exponent" is employed in addition to the "Perturbation Scale" to see the behavior of the algorithm obtaining the optimum result. Similar to the first case, it was not able to find an improved solution over the default setting of SA.

REFERENCES

Aboudi, Jacob, Steven Arnold, and Brett Bednarcyk. 2013. *Micromechanics of Composite Materials*. *Micromechanics of Composite Materials*. https://doi.org/10.1016/C2011-0-05224-9.

Ahmad, Sameer, and Leeladhar Rajput. 2020. "Buckling Analysis of Inter-Ply Hybrid Composite Plate." *Materials Today: Proceedings* 21: 1313–19. https://doi.org/10.1016/j.matpr.2020.01.168.

Andhini, Nisa Fitri. 2017. "Composite Technologies for 2020." *Journal of Chemical Information and Modeling* 53 (9): 1689–99.

António, Carlos Conceição, and Luísa Natália Hoffbauer. 2016. "Bi-Level Dominance GA for Minimum Weight and Maximum Feasibility Robustness of Composite Structures." *Composite Structures* 135: 83–95. https://doi.org/10.1016/j.compstruct.2015.09.019.

Aymerich, F., and M. Serra. 2008. "Optimization of Laminate Stacking Sequence for Maximum Buckling Load Using the Ant Colony Optimization (ACO) Metaheuristic." *Composites Part A: Applied Science and Manufacturing* 39 (2): 262–72. https://doi.org/10.1016/j.compositesa.2007.10.011.

Baba, Buket Okutan. 2007. "Buckling Behavior of Laminated Composite Plates." *Journal of Reinforced Plastics and Composites* 26 (16): 1637–55. https://doi.org/10.1177/0731684407079515.

Charkviani, Ramaz V., Alexander A. Pavlov, and Svetlana A. Pavlova. 2017. "Interlaminar Strength and Stiffness of Layered Composite Materials." *Procedia Engineering* 185: 168–72. https://doi.org/10.1016/j.proeng.2017.03.335.

Claassen, J. H. 2009. “FEM Analysis of Magnetic Flake Composites.” *Journal of Magnetism and Magnetic Materials* 321 (14): 2166–69. https://doi.org/10.1016/j.jmmm.2009.01.020.

Dahal, Raj Kumar, Bishnu Acharya, Gobinda Saha, Rabin Bissessur, Animesh Dutta, and Aitazaz Farooque. 2019. “Biochar as a Filler in Glassfiber Reinforced Composites: Experimental Study of Thermal and Mechanical Properties.” *Composites Part B: Engineering* 175 (March): 107169. https://doi.org/10.1016/j.compositesb.2019.107169.

Deveci, H. Arda, Levent Aydin, and H. Seçil Artem. 2016. “Buckling Optimization of Composite Laminates Using a Hybrid Algorithm under Puck Failure Criterion Constraint.” *Journal of Reinforced Plastics and Composites* 35 (16): 1233–47. https://doi.org/10.1177/0731684416646860.

Duffy, K. J., and S. Adali. 1990. “Design of Antisymmetric Hybrid Laminates for Maximum Buckling Load: II. Optimal Layer Thickness.” *Composite Structures* 14 (2): 113–24. https://doi.org/10.1016/0263-8223(90)90026-B.

Duran, A. V., N. A. Fasanella, V. Sundararaghavan, and A. M. Waas. 2015. “Thermal Buckling of Composite Plates with Spatial Varying Fiber Orientations.” *Composite Structures* 124: 228–35. https://doi.org/10.1016/j.compstruct.2014.12.065.

Erdal, Ozgur, and Fazil O. Sonmez. 2005. “Optimum Design of Composite Laminates for Maximum Buckling Load Capacity Using Simulated Annealing.” *Composite Structures* 71 (1): 45–52. https://doi.org/10.1016/j.compstruct.2004.09.008.

Fontes, Raphael Siqueira, Hallyjus Alves Dias Bezerra, Ana Claudia Melo De Caldas Batista, Sérgio Renan Lopes Tinôa, and Eve Maria Freire De Aquino. 2019. “Failure Theories and Notch Type Effects on the Mechanical Properties of Jute-Glass Hybrid Composite Laminates.” *Materials Research* 22 (2). https://doi.org/10.1590/1980-5373-MR-2018-0269.

Huang, Qianli, Shenghang Xu, Zhengxiao Ouyang, Yan Yang, and Yong Liu. 2021. "Multi-Scale Nacre-Inspired Lamella-Structured Ti-Ta Composites with High Strength and Low Modulus for Load-Bearing Orthopedic and Dental Applications." *Materials Science and Engineering C* 118 (May 2020): 111458. https://doi.org/10.1016/j.msec.2020.111458.

Karakaya, Şükrü, and Ömer Soykasap. 2009. "Buckling Optimization of Laminated Composite Plates Using Genetic Algorithm and Generalized Pattern Search Algorithm." *Structural and Multidisciplinary Optimization* 39 (5): 477–86. https://doi.org/10.1007/s00158-008-0344-2.

Modniks, J., and J. Andersons. 2010. "Modeling Elastic Properties of Short Flax Fiber-Reinforced Composites by Orientation Averaging." *Computational Materials Science* 50 (2): 595–99. https://doi.org/10.1016/j.commatsci.2010.09.022.

Onal, Gurol. 2006. "Mechanical Buckling Behavior of Hybrid Laminated Composite Plates with Inclined Crack." *Journal of Reinforced Plastics and Composites* 25 (14): 1535–44. https://doi.org/10.1177/0731684406066750.

Plagianakos, V P, G D Magoulas, and M N Vrahatis. n.d. "Chapter 15 IMPROVED LEARNING OF NEURAL NETS."

Riche, Rodolphe Le, and Raphael T. Haftka. 1993. "Optimization of Laminate Stacking Sequence for Buckling Load Maximization by Genetic Algorithm." *AIAA Journal* 31 (5): 951–56. https://doi.org/10.2514/3.11710.

Sadowski, Tomasz, Patrizia Trovalusci, Bernhard Schrefler, and René de Borst. 2014. "Multi-Scale and Multi-Physics Modelling for Complex Materials." *Meccanica* 49 (11): 2549–50. https://doi.org/10.1007/s11012-014-0040-9.

Savran, Melih, and Levent Aydin. 2018. "Stochastic Optimization of Graphite-Flax/Epoxy Hybrid Laminated Composite for Maximum Fundamental Frequency and Minimum Cost." *Engineering Structures* 174 (July): 675–87. https://doi.org/10.1016/j.engstruct.2018.07.043.

Soykasap, Omer, and Şükrü Karakaya. 2007. “Structural Optimization of Laminated Composite Plates for Maximum Buckling Load Capacity Using Genetic Algorithm.” *Key Engineering Materials* 348–349: 725–28. https://doi.org/10.4028/www.scientific.net/kem.348-349.725.

Tawfik, Basem E., Heba Leheta, Ahmed Elhewy, and Tarek Elsayed. 2017. “Weight Reduction and Strengthening of Marine Hatch Covers by Using Composite Materials.” *International Journal of Naval Architecture and Ocean Engineering* 9 (2): 185–98. https://doi.org/10.1016/j.ijnaoe.2016.09.005.

Wankhade, Rajan L., and Samiksha B. Niyogi. 2020. “Buckling Analysis of Symmetric Laminated Composite Plates for Various Thickness Ratios and Modes.” *Innovative Infrastructure Solutions* 5 (3): 0–12. https://doi.org/10.1007/s41062-020-00317-8.

Yeter, Eyüp, Ahmet Erkliğ, and Mehmet Bulut. 2014. “Hybridization Effects on the Buckling Behavior of Laminated Composite Plates.” *Composite Structures* 118 (1): 19–27. https://doi.org/10.1016/j.compstruct.2014.07.020.